

# Surface charge driven polymeric drug carrier for bone specific delivery of estradiol: in vitro and in vivo assessment

**Meenakshi Venkataraman**

Bombay College of Pharmacy

**Bhabani Mohanty**

Advanced Centre for Treatment Research and Education in Cancer

**Pradip Chaudhari**

Advanced Centre for Treatment Research and Education in Cancer

**Darshan Kumar**

University of Helsinki Department of Biosciences: Helsingin yliopisto Bio- ja ymparistotieteellinen tiedekunta

**Mangal S. Nagarsenker** (✉ [mangal.nagarsenker@gmail.com](mailto:mangal.nagarsenker@gmail.com))

Bombay College of Pharmacy

---

## Research Article

**Keywords:** osteoporosis, polymeric nanoparticles, estradiol, bone diseases, cationic nanoparticles, polyethylene imine

**Posted Date:** February 16th, 2022

**DOI:** <https://doi.org/10.21203/rs.3.rs-1314880/v1>

**License:** © ⓘ This work is licensed under a Creative Commons Attribution 4.0 International License.

[Read Full License](#)

---

# Abstract

Osteoporosis is a systemic skeletal disease affecting postmenopausal women worldwide. Adverse side effects are associated with long term conventional hormone therapy in osteoporosis treatment. Estradiol was loaded in PLGA nanoparticles coated with polyethylene imine to impart positive surface charge to preferentially localize hormone in the negative surface of bone environment evading unwanted side effects. Nanoparticles prepared by emulsion solvent evaporation method were smaller than 200 nm with a surface charge of 35mV. In vitro hydroxyapatite binding studies revealed superior binding of 82% by polycationic particles compared to meagre 28% by plain PLGA nanoparticles. In vivo biodistribution studies in mice displayed nearly 3 fold higher bone uptake by cationic nanoparticles compared to plain PLGA system at 24 hours. Hematological and histological evaluation in acute toxicity study showed safe and nontoxic nature of cationic nanoparticles.. Higher  $C_{max}$ ,  $AUC_{0-inf}$ ,  $t_{1/2}$  values and lower clearance values was observed with nanoparticles compared to estradiol solution which can potentially lower frequency of administration compared to plain drug solutions. The osteoprotective effect of estradiol in cationic nanoparticles was established in ovariectomised rats. The osteotropic, nontoxic cationic nanoparticles can be considered a prototype for delivery of plethora of antiresorptive/anabolic agents to the skeletal environment.

## 1. Introduction

Bone is metabolically active, highly organized rigid skeleton playing vital role in calcium and phosphate homeostasis (Kong et al,1997). It undergoes constant lifelong remodeling activity to maintain skeletal integrity, shape and mass which are regulated by hormones such as estrogen, calcitonin, Osteoclasts, bone resorbing cells and osteoblasts, bone building cells regulate the process together and play a significant role in maintenance of healthy bone environment (Pivonka ,Zimak, 2008; **Shea and Miller 2005**). An offset in this balance results in a number of serious bone disorders such as osteopetrosis, Paget's disease.

Osteoporosis is a systemic skeletal disease characterized by low bone mass attributed to the over activity of osteoclasts and the concurrent inability of osteoblasts to reconstitute the resulting bone loss. This debilitating bone disorder is highly prevalent in post menopausal women worldwide (Peterlik,1997). One of the prominent etiologies for osteoporosis is the deficiency of estrogen, a female hormone. Estrogen supplementation in postmenopausal condition decreases the formation and activity of osteoclasts and reverses the activation frequency to premenopausal level (Ji and Yu, 2015). This female hormone reportedly affects resorption by direct action on osteoclast progenitors thereby preventing the formation of osteoclasts. Estrogen plays a significant role in controlling osteoclast number, activity and life span in a paracrine manner (Khosla, Oursler, 2012). The existing medical intervention entails continuous oral estradiol medication for 3-5 years. However recently major life threatening risks such as ovarian cancer, endometrium cancer, breast cancer, stroke associated with this long term conventional estrogen therapy have been reported in aging females (Yoo and Lee, 2006). The extensive indiscriminate distribution and activity in non-skeletal organs especially in reproductive tissues curtails the availability of estrogen in

local bone environment thereby resulting in increased unwanted systemic activity in females. This strongly suggests the need for novel bone targeting drug delivery system with low estradiol dose exhibiting maximum pharmacological therapeutic effect in the peripheral site consequently evading deleterious side effects in long term post menopausal osteoporosis therapy. Targeting nanoparticles to bones is as hard as the target tissue itself. Maintaining essential optimum drug levels at the site of action for desired therapeutic effect is a major challenge. Bones are poorly vascularized and distributed throughout body. Moreover, the presence of bone marrow-blood barrier refrains free entry of large exogenous molecules in bone environment (Hirabayashi and Fujisaki 2003). Spatial targeting using active biomolecules is one of the pragmatic strategies to improve therapeutic index and reduce the adverse side effects of these therapeutic agents. The lack of expression of specific enzymes, antigens in bone environment impedes the scope of ligand oriented targeting.

Hydroxyapatite, a predominant component of extracellular mineralized bone matrix, accounts for nearly 69% by weight of fresh bone (Wang, Miller et al, 2005). Hydroxyapatite is an assemblage of oppositely charged ions viz;  $\text{Ca}_{10}(\text{PO}_4)_6(\text{OH})_2$  and bears a slightly negative charge at physiological conditions with the point of zero charge, pH 7.3 (Zhang, Wright et al. 2007). This condition is favorable to bind positively charged molecules such as lysozyme, polymers like polyethyleneimine, poly L lysine via electrostatic interactions. The skeletal abundance and exclusivity of hydroxyapatite offers opportunity for charge driven polymeric carriers to localize drug molecules preferentially in bone milieu.. In a study by Zhang et al cationic polymers, polyethyleneimine/poly L lysine exhibited strong binding to hydroxyapatite (Zhang, Wright et al. 2007).

Polymeric systems have the potential to house an array of molecules with diverse physicochemical properties prescribed in treatment of many skeletal disorders. Exhaustive research in polymer therapeutics has led to the development of nanosystems with varied architectures and properties (Mitchell, Billingsley et al, 2021). A plethora of research papers on polymeric nanoparticles warrants its wide application. Polymeric nanotechnology encompasses development of multifaceted biocompatible nanosystems which find use in diagnostics and therapeutic areas. Biocompatible polymers such as PLGA have been extensively explored as drug carriers (Jose, Cinu et al, 2019; Gu, Wusiman et al 2019; Shahzad, Naeem et al, 2019). Controlled drug delivery, improved solubilisation of drug, enhancement of bioavailability, storage and enzymatic stability are some added advantages of these nanosystems. Taking into account the benefits of polymeric carrier systems and promising role of cationic polymer PEI in bone targeting, it was considered worthwhile to evaluate PLGA nanoparticles coated with PEI as carriers for bone targeted drug delivery of estradiol.

This research paper describes development and optimization of estradiol loaded PLGA nanoparticles coated with PEI (PNP). Nanoparticles were prepared by emulsion solvent evaporation method and were characterised with respect to particle size, entrapment efficiency, surface charge. Estradiol release from polymeric carrier was determined in vitro using modified dialysis method and in vivo in Sprague Dawley rats using suitable bioanalytical method. In vivo acute toxicity studies were performed to ensure the safety of PEI coated nanoparticles. The bone targeting potential was validated in vitro with

hydroxyapatite suspension and further assessed by invasive and non invasive biodistribution studies in swiss albino mice. The osteoprotective effect of estradiol in cationic nanoparticles was established in ovariectomised rats. The osteotropic, nontoxic nature of novel cationic nanoparticles developed have the potential to house diverse drug molecules prescribed in treatment of bone disorders and find a prominent role in bone targeted therapy.

## **2. Materials**

Estradiol and Polyethyleneimine (PEI) 5KDa linear polymer were purchased from Sigma Aldrich. PLGA (50:50) Resomer rg 504H was procured from Evonik Healthcare Ltd. Poloxamer 188 was a gift sample from BASF. Dichloromethane, methanol were procured from S D Fine chemicals. Solvents used were of analytical grade.

## **3. Method**

### **3.1. Preparation of polymeric nanoparticles**

Nanoparticles were prepared by emulsion solvent evaporation method. Briefly, PLGA, PEI and estradiol was dissolved in organic phase comprised of a homogenous mixture of dichloromethane and methanol. Poloxamer 188, stabilizing agent was solubilized in water and organic phase was added to stabilizer solution drop wise under shear using high speed homogenizer (IKA T10, Ultra turrax) to give coarse oil in water primary emulsion. An organic to aqueous ratio was 1:5. The coarse emulsion was further subjected to sonication at 40% amplitude for 6 minutes using a probe sonicator (Branson Digital Sonifier, US). Furthermore, the solvent was evaporated under reduced pressure using rotary evaporator (Roteva Mumbai) to give nanoparticle dispersion. Plain conventional PLGA nanoparticles (CNP) were prepared using the same procedure, excluding PEI. Estradiol loaded nanoparticulate dispersion was freeze dried in lyophiliser (Labconco India Pvt Ltd) with 10%w/v trehalose as a cryoprotectant.

### **3.2.Characterisation**

#### **3.2.1. Particle size and polydispersity index**

The particle size was measured on N5 Beckman Coulter Sub micron Particle Size analyzer, (Beckman Coulter, USA) which works on the principle of photon correlation spectroscopy (PCS). All experiments were carried out at 25° C using disposable polystyrene cells, after appropriate dilution with Milli-Q Type I water (Merck Millipore Pvt Ltd, Germany). Measurements were carried out at 90<sup>0</sup> at 25<sup>0</sup> C. Dispersions were diluted with Milli-Q Type I water to ensure that the light scattering intensity was within the instrument's sensitive range.

#### **3.2.2. Entrapment efficiency**

Nanoparticles were diluted with Milli-Q Type I water and centrifuged at 80,000 rpm for 1h (Beckmann Ultracentrifuge, USA). The pellet was appropriately diluted with methanol and absorbance was measured using a suitable analytical method. Empty nanoparticles were treated as blank. Entrapment efficiency was calculated as follows,

$$\text{Percent Entrapment Efficiency} = \frac{\text{Amount of drug in nanoparticles}}{\text{Amount of drug added}} \times 100$$

### 3.2.3. Surface charge

Surface charge of PLGA and cationic nanoparticles were determined using Malvern Zetasizer, Nanoseries Nano ZS (UK). The samples were appropriately diluted with Milli-Q Type I water (Merck Millipore Pvt Ltd, Germany) and surface charge was measured using clear disposable zeta cell-DTS 1060 C (Malvern, UK).

### 3.2.4. In vitro hydroxy apatite (HA) targeting ability

Bone targeting potential of nanoparticles was evaluated by analyzing their binding to hydroxy apatite (HA). HA was suspended in phosphate buffer pH 7.4 to yield 500mg/mL concentration. Nanoparticle dispersion was mixed with HA suspension and then gently shaken for 1 h at room temperature (Remi waterbath shaker, Mumbai). This was then centrifuged at 5000 rpm for 10 minutes. The supernatant was diluted with methanol and analyzed for drug content.

### 3.2.5. Cryo TEM

Morphology of cationic PLGA nanoparticles were studied by cryo tem. Three microliters of each sample was applied onto Quantifoil R 2/2 grids and vitrified in liquid ethane with Leica EMGP vitrification device. The cryo-TEM data collection was performed under low-dose conditions with Gatan 626 cryo-holder and a FEI Tecnai F20 microscope operated at 200 keV. Electron micrographs were recorded with a Gatan Ultrascan 4000 charge-coupled-device (CCD) camera at a magnification of  $\times 69000$  and a 5.0  $\mu\text{m}$  nominal underfocus.

### 3.2.6. Thermal Analysis- Differential Scanning Calorimetry (DSC)

Thermal behavior of estradiol in pure form and in cationic polymeric nanoparticle was determined using DSC (Mettler Toledo DSC 1 Switzerland). The samples were subjected to heat at  $10^{\circ}\text{C}/\text{min}$  in nitrogen environment. The heating cycle was in the range  $25^{\circ}$  to  $250^{\circ}\text{C}$ .

### 3.2.7. In vitro release study

In vitro release behavior of novel nanoformulations was investigated using dialysis membrane modified USP type I apparatus (Electrolab dissolution apparatus, Mumbai) for 48 h at a rotation speed of 100 rpm. In vitro release of estradiol from solution, EST PLGA nanoparticles, EST cationic nanoparticles was evaluated in 30% ethanol in PBS pH 7.4 to maintain sink conditions. Samples (1 mL) were filled in

dialysis bag tied to the shaft of the basket-type dissolution apparatus after detaching the basket at the end of the shaft. An aliquot of 1 ml dissolution medium was removed at a series of various points (0.5, 1, 2, 4, 6, 8, 10, 12, 24 and 48 h) and the same volume of fresh release medium was replaced. Drug content in aliquots were analyzed by appropriate HPLC method and percent cumulative release was calculated. Statistical analysis of release data was performed using Student's unpaired t test.  $P \leq 0.05$  was considered significant.

The mechanism of release was determined by fitting the release data obtained in different kinetic drug-release models such as zero order, Higuchi and Korsmeyer Peppas. Regression coefficient ( $R^2$ ) was calculated from plots and the value closest to 1 was considered as a best fit model.

### **3.2.8. In vivo Pharmacokinetic study**

In vivo pharmacokinetic study was performed in female Sprague Dawley rats. The protocol was approved by Institutional Animal Ethics Committee of Bombay College of Pharmacy, Mumbai, India. Rats (200-250 g) were purchased from Bombay Veterinary College, Parel, and the animals were quarantined at  $25^0 \pm 2^0$  C in a 12 h dark/light cycle and food ad libitum. Animals were divided in 3 groups of eight animals each and received EST solution, EST loaded PLGA nanoparticles and Estradiol loaded cationic PEI coated polymeric nanoparticles. All the formulations were administered intravenously via tail vein at estradiol dose of 1 mg/kg. Blood samples (0.5 mL) were collected in EDTA (1 mg/0.1mL) on retro-orbital puncture. Samples were withdrawn under mild anesthesia at 0.5, 1, 2, 4, 6, 8, 10, 12, 24 h. Four out of eight animals in each group were used for alternate time points and at each consecutive time blood was withdrawn from the alternate eye. Plasma was separated by centrifuging heparinized blood at 8000 rpm (Minispin centrifuge, Eppendorf, Germany) for 5 minutes and stored  $-20^0$  C till further analysis. Samples were analysed for drug content using validated bioanalytical method. The pharmacokinetic parameters were calculated using the PKSolver 2.0 add-in for Excel using compartmental analysis.

### **3.2.9. In vivo toxicity study**

Swiss albino mice were purchased from Bombay Veterinary College, Mumbai. Animals were divided into 2 groups of 6 animals each. Control group was treated with saline. Single dose of cationic polymeric nanoparticle was administered intravenously to the other group. Animals were observed for 14 days for any mortality or abnormality. At the end of 14 days, animals were sacrificed and hematological parameters were evaluated. Vital organs like liver, lung, kidney, heart, spleen, ovaries, bones were weighed and investigated for histopathological abnormality. Statistical analysis of organ weight data was performed using Student's unpaired t test.  $P \leq 0.05$  was considered significant.

### **3.2.10. In vivo biodistribution study-**

#### **3.2.10.1. Radiolabelling of nanoparticles**

Briefly, 18.8  $\mu$ L stannous chloride solution (10 mg/mL in glacial acetic acid) was added to 2mCi pertechnatate sodium followed by 0.5 mL formulation dispersion. The radioactivity was measured using

dose calibrator (CRC 15R, Capintec Inc., USA). The mixture was incubated at 37<sup>0</sup> C for 15 minutes. The pH was adjusted to neutral using 0.5 M NaHCO<sub>3</sub> solution. The radiolabelling efficiency as determined by thin layer chromatography. Acetone was used as mobile phase and silica was the stationary phase. Radioactive counts in different sections of TLC plate were determined using gamma counter.

Radiolabelling efficiency was calculated using the following formula

$$\text{Total radiocounts} - \text{Free Technetium counts}$$

$$\text{Radiolabelling efficiency} = \frac{\text{Total radiocounts} - \text{Free Technetium counts}}{\text{Total radiocounts}} \times 100$$

Total radiocounts

### 3.2.10.2. Invasive and non invasive evaluations

The experiments were conducted in healthy female Swiss albino mice in the weight range of 25-30 g (n=3/ formulation and time point). Optimised radiolabelled formulations were injected intravenously via tail vein at a dose of nearly 700 $\mu$ Ci 99m Tc under isoflurane anesthesia.

#### Invasive Study

In case of invasive study, animals were sacrificed using cervical dislocation at 1h, 5h, 24h post dosing. Vital organs like bones, heart, kidneys, brain, stomach, gut, RES organs, representative blood samples were isolated. Radioactive counts in these organs were read using a gamma counter and percent injected dose per gram tissue was calculated.

#### Non Invasive Study

CT and SPECT images of mice were recorded using gamma camera (Model SYS000002 Elgems MilleniumVG, WI, USA) auto tuned to detect 140 keV radiation of 99 mTc post formulation administration. Animals were under isoflurane anesthesia throughout the scanning procedure

### 3.2.11. In vivo efficacy study

Female Sprague Dawley rats were procured from National Institute of Biosciences, Pune. Rats were housed in cages at 25<sup>0</sup>  $\pm$  2<sup>0</sup> C in a 12 h dark/light cycle and fed food and water ad libitum. They were acclimatized for a period of 1 week. The study was performed on 12 week old rats weighing 200-250 g. Seven animals were sham operated. The rest of 28 animals were ovariectomized under ketamine and xylazine anesthesia. These animals were randomly divided into 4 groups (n=7).

1. Treated with EST loaded cationic nanoparticles
2. Treated with EST loaded PLGA nanoparticles
3. Treated with EST solution
4. OVX control (negative control)

The surgical wound was allowed to heal prior to the commencement of therapy. Animals were treated twice a week for eight weeks. All the formulations were administered intravenously via tail vein at estradiol dose of 1 mg/kg. Blood samples (0.5 mL) were collected on retro-orbital puncture. After the rats were sacrificed, tibia and femur were isolated and stored at  $-80^{\circ}\text{C}$  for further evaluation. The biochemical parameters such as serum calcium, phosphorus and alkaline phosphatase levels were assessed using biochemical kits obtained from Erba Diagnostics Mannheim. Bone density was determined by Archimedes principle reported by Gupta et al (Gupta, Goyal et al.2014). Briefly, bones were submerged in water and their weights were recorded. Bones were removed from water and weighed. Bone density was determined using the following formula. Bone density =  $(A/A - B)$ , where, A: weight of hydrated bone out of water, B: weight of hydrated bone submerged in water, and  $A - B$ : difference in weight of bone, which is equivalent to the volume. Bone strength was assessed by the endurance exhibited by bone on subjecting a force longitudinally using Monsanto hardness tester indicated by hardness values. Comparisons between different treatments were analyzed by one-way ANOVA followed by Tukey's multiple comparison tests ( $P < 0.05$ ) using GraphPad Prism.

## 4. Results And Discussion

Nanoparticles are well established, most efficient, versatile drug carrier systems. Estradiol was entrapped in cationic PLGA nanoparticles stabilized by poloxamer 188. PLGA-Poloxamer 188, a well-established polymer-stabilizer combination, has proven to yield stable nanoparticles harboring an array of molecules with differing physiochemical properties such as docetaxel (Yan, Zhang et al. 2010). doxorubicin (Gelperina, Maksimenko et al. 2010), 5-fluorouracil (Li, Xu et al. 2008). Poloxamer 188 was evaluated at 0.5% and 1% w/v concentration as a stabilizer for estradiol PNP. Estradiol, a steroidal hormone with a log P value of 4, is expected to be solubilized in the hydrophobic PLGA matrix of the nanoparticle. With a view to attain stable nanosystems with superior estradiol loading, two different PLGA proportions viz. 1%w/v and 2%w/v were assessed. It is imperative to impart positive surface charge for superior hydroxy apatite binding concurrently evading potential cytotoxic effects which are associated with cationic polymers like PEI. Therefore, low molecular weight (5000 Da) linear PEI was used at 0.25%w/v and 0.5%w/v concentration to confer the necessary cationic surface charge.

The method of preparation is governed by the properties of the drug molecule and the polymers employed. In the present work, estradiol loaded cationic nanoparticles were prepared by emulsion solvent evaporation technique. Owing to the differing solubilities of the polymers in organic solvents, PLGA and PEI were solubilized in organic phase comprised of a DCM and methanol.. Poloxamer 188 was dissolved in the aqueous phase. Primary coarse o/w emulsion was obtained on addition of organic phase to aqueous phase in 1:5 ratio under shear at a maximum speed of 30000 rpm, by high speed homogenizer (IKA, Ultra Turrax,Mumbai). Further nanosizing of the oil droplets was attained on probe sonication. Removal of solvents from nanoemulsion under vacuum resulted in nanoprecipitation of estradiol loaded polymers in aqueous phase. The effect of formulation factors was assessed to determine an optimized formula.

## 4.1. Particle size and polydispersity index

Emulsification and stabilization are predominant factors controlling particle size and stability of nanoparticles. A number of reports in literature suggest stabilisation of PLGA nanoparticles with poloxamer 188. Formula P1 and P2 prepared with 1% and 2% w/v PLGA respectively were stabilized by 0.5% w/v poloxamer 188 (table.1). The mean particle size and PI increased from 135 nm to 204 nm and 0.35 to 0.39 respectively with an increment in PLGA content. On increasing the stabilizer proportion to 1% w/v in P3 and P4, smaller particles were obtained. This implied that the amount of stabilizer played a crucial role. In an emulsion, surfactant molecules align themselves at the interface, lowering the free energy thereby inhibiting coalescence of droplets. Solvent removal from droplets yields stable nanoparticles. Higher content of poloxamer 188 was vital to stabilize large surface area of nanodroplets in emulsion obtained with higher amount of PLGA.

Table 1  
Effect of stabilizer with (Nanoparticles with 0.5% PEI content)

Formulation	PLGA % w/v	Poloxamer 188 (% w/v)	Particle Size (nm)	Polydispersity index
P1	1	0.5	135 ± 2.3	0.35 ± 0.06
P2	2	0.5	204 ± 22	0.39 ± 0.04
P3	1	1	127 ± 1.7	0.26 ± 0.07
P4	2	1	178 ± 2.1	0.240 ± .03
n=3				

## 4.2. Entrapment efficiency

Estradiol, a hydrophobic molecule is assumed to solubilize in amorphous PLGA matrix. The amount of carrier PLGA available for lodging estradiol plays a crucial role in governing entrapment. Estradiol was loaded at a maximum of 10% w/w of PLGA in PNP. Higher PLGA content is expected to increase the solid state solubility of estradiol in matrix. The entrapment efficiency of was 75-80% (table. 2). This was superior to that of values reported by Mittal et al which was 67%. (Mittal, Sahana et al. 2007). This discrepancy could be explained by the difference in grade and source of PLGA, organic to aqueous ratio, shear force applied, rate of solvent evaporation, factors which govern estradiol partitioning to the organic polymeric phase.

Table. 2. Effect of estradiol: PLGA proportion on entrapment efficiency.

(Nanoparticles with 0.5% w/v PEI and 1% w/w poloxamer 188)

Formulation	PLGA % w/v	Estradiol (%polymer content)	Entrapment efficiency
P5	1	5	75.6 ± 2.4
P6	1	10	77.12 ± 3.4
P7	2	5	79.4 ± 1.9
P8	2	10	78.78 ± 2.5
n=3			

### 4.3. Surface charge

PEI is the significant component in PNP responsible to bestow positive charge. Surface charge of nanoparticles with and without PEI is as depicted in Fig. 1. Negative zeta potential of -11 mV was observed with plain PLGA nanoparticles. Formulations with 0.25% w/v and 0.5% w/v PEI showed zeta potential values of +28 and +35 mV respectively. This increase in the surface charge confirms the presence of polycationic polymer, PEI on the surface of nanoparticle. The positive charge increased with proportion of PEI. The high zeta potential value observed in our investigation indicates good colloidal stability and is expected to have profound influence in bone binding property.

### 4.4. In vitro hydroxy apatite (HA) binding efficiency

In vitro HA binding of polymeric nanoparticles with and without PEI was evaluated. Figure 1.2 depicts HA binding affinity of different PNP formulations. As mentioned earlier, an increase in positive charge was observed with increase in PEI concentration. Plain PLGA nanoparticles without PEI showed meager 28% binding efficiency (Fig. 2.). On the contrary nanoparticles bearing PEI on their surface displayed superior binding of 82%. At physiological conditions, bone surface bears negative charge. The electrostatic interactions between negative surface and positive particle is expected to result in strong binding. This result affirms the findings by Zhang et al (Zhang, Wright et al. 2007). Taking into account potential cytotoxicity of PEI at high doses, and remarkable binding results in in vitro experiments, 0.5%w/v PEI concentration was considered optimum.

Based on the results it was construed that at 0.5% w/v of PEI concentration, 1% w/v of poloxamer 188 and 2% w/v PLGA yields positively charged nanoparticles desirable for strong binding of PNP to bone surface.

### 4.5. Cryo TEM

Morphological evaluation of PEI coated PLGA nanoparticles revealed their dense spherical structure. The solid core represents PLGA matrix with estradiol. The lighter layer on the outer surface surrounding the particle could be attributed to the coating with PEI and poloxamer 188. The particles in images appear smaller with 100-110 nm size (Fig. 3.) compared to the 178 nm obtained on assessment with particle size analyser. Photon correlation spectroscopy analyser works on dynamic light scattering principle which

measures hydrodynamic diameter of the dispersed particles additionally accounting for the water layer surrounding nanoparticle surface. Whereas in cryotem, the morphology and particle size of frozen particles per se is determined. Moreover, the number distribution of particles assessed in analyser is larger than in cryo tem thus reflecting polydispersity of the sample. Similar disparity in particle size was also observed in few reports (Venkataraman and Nagarsenkar, 2013 ).

## 4.6. Thermal analysis

In the present investigation, EST drug sample and EST nanoparticles were subjected to heat cycle at 10<sup>0</sup> C per min rate. Crystalline nature of pure estradiol was evident from the sharp melting peak at 178<sup>0</sup> C (Fig. 4). Absence of this peak in nanoparticle sample indicates estradiol solubilisation in PLGA matrix. It is anticipated that hydrophobic molecule EST remains in an amorphous solubilized state in hydrophobic PLGA matrix similar to the findings reported Musumeci et al (Musumeci, Ventura et al. 2006).

## 4.7. Freeze drying

Freeze drying is a promising approach for the stabilisation of colloidal dispersions. In the case of PLGA nanoparticles, the hydrolytic instability of the polymer in aqueous dispersion is the main issue. PNP dispersion was freeze dried to improve its stability for long term storage. Trehalose was used as a cryoprotectant at 10% w/v. The visual inspection of the lyophilised products did not show any signs of collapse or shrinkage after the freeze drying process. The freeze dried cakes were brittle and easy and rapid to reconstitute (table. 3).

Table 3

Particle size, surface charge and entrapment efficiency post rehydration of lyophilized product

Formulation	Mean particle size (nm)	Polydispersity index	Surface charge (mV)	Entrapment efficiency (%)
PNP dispersion	178	0.24	33.32	78.78
Freeze dried PNP (10% w/v trehalose) (rehydrated)	181	0.26	34.79	79.32

## 4.8. In vitro release studies.

PLGA nanoparticles are well established systems for sustained release of drug in vivo. A number of factors such as the ratio of lactide- glycolide, particle size, exposure to release medium (surface area and shape), temperature, degradation rate of PLGA, govern drug release from the matrix. In non targeted conventional PLGA nanoparticles (CNP), estradiol is entrapped in polymeric matrix composed of PLGA (50:50) Resomer rg 504H with equal portions of fast degrading, hydrophilic PGA and slow degrading hydrophobic PLA. EST loaded PLGA nanoparticles released EST only to an extent of 40% in 48 hours (Fig. 5.) compared to a faster release of 85% observed from solution. (P<0.05). This sustained effect is

owing to the slow erosion and subsequent dissolution of EST from PLGA matrix. In case of bone targeted cationic PEI coated nanoparticles (PNP), 33% EST released in 48 h which was slower than plain PLGA nanoparticles (CNP). This could be attributed to the presence of additional PEI polymeric barrier on nanoparticle surface, hampering EST release from nanoparticles. EST release from PLGA nanoparticles reported for oral delivery also exhibited sustained release (Mittal, Sahana et al. 2007). Sustained EST release from PLGA nanoparticles can potentially reduce systemic drug levels, thereby releasing and maintaining therapeutic EST levels in the bone milieu reducing the dosing frequency in osteoporosis therapy.

Drug release from nanoparticles can follow a number of mechanisms. The drug release could be due to PLGA degradation which leads to erosion of matrix alongwith, diffusion mediated dissolution of drug from nanoparticles. Though these mechanisms work in harmony, their rates vary. With a view to identify the predominant mechanism, release data was fitted into various kinetic models. Graphs of cumulative percent drug release vs time (zero order), log percent drug remaining vs time (first order), cumulative percent drug release vs square root of time (Higuchi), cube root of percent drug remaining vs time (Hixson Crowell) and log percent drug release vs log time (Korsmeyer Peppas) were plotted. Table 4. summarizes the correlation values for these models. The best fit model was Korsmeyer peppas with highest correlation value of 0.98.

This clearly indicates that EST release from nanoparticle is primarily governed by diffusion mechanism. The magnitude of the release exponent value ( $n$ ) < 0.43 implies that the release follows fickian diffusion mechanism. As the polymer degrades/erodes with time, the particle size of nanoparticles decrease. This increase in surface area and concentration gradient further stimulates drug release. On the contrary increased membrane thickness attenuates drug release resulting in sustained effect.

Table 4  
Summary of correlation values for release kinetic models

	Zero	First	Higuchi	Hixson Crowell	Korsmeyer Peppas	
	R <sup>2</sup>	R <sup>2</sup>	R <sup>2</sup>	R <sup>2</sup>	N	R <sup>2</sup>
EST CNP	0.9760	0.9392	0.9729	0.9689	<b>0.0983</b>	<b>0.9773</b>
EST PNP	0.9489	0.921	0.9489	0.9333	<b>0.1143</b>	<b>0.9646</b>

## 4.9. Pharmacokinetic studies

Pharmacokinetic profiles of EST solution, conventional and bone targeted polymeric systems obtained are as shown in Fig. 6 depicts drug plasma levels. EST solution followed one compartmental kinetics whereas both nanoparticles followed 2 compartmental kinetics with good relation between predicted and observed values. The  $r^2$  value was more than 0.97 for all systems. Two compartmental kinetics implies biexponential decline in plasma levels with nanosystems as opposed to single exponential plasma level

reduction seen with solution. Post intravenous administration of solution, drug levels dropped drastically and were undetectable after 6 hours. Plasma levels of EST from conventional (CNP) and bone targeted polymeric nanoparticles (PNP) were 689 ng/mL and 824.15 ng/mL respectively at 30 minutes as shown in Fig. 6 Interestingly, there was no statistically significant difference in drug plasma levels observed with conventional and bone targeted nanosystems. The distribution of targeted systems to less perfused organ bone, and subsequent binding is not expected to reflect significantly in plasma drug levels.

EST was rapidly cleared from solution. Clearance and AUC<sub>0-inf</sub> values obtained for EST solution were 0.54 (µg)/(ng/ml)/h and 458.87 ng/ml\*h respectively. In case of conventional (CNP) and bone targeted nanoparticles (PNP) the clearance values significantly reduced to 0.061 and 0.057 (µg)/(ng/ml)/h whereas AUC<sub>0-inf</sub> values substantially increased to 7022.61

and 14311.71 ng/mL\*h respectively (Table 5). This trend is similar to the pharmacokinetic data of sustained release nanosystems reported in literature (Patere, Pathak et al, 2016). Based on invitro release studies and in vivo pharmacokinetic data, it can be construed that polymeric nanosystems exhibit sustained release of EST which has potential for lowering frequency of administration compared to plain drug solution. This is expected to reduce the adverse side effects associated with the long term exposure of EST to organs in conventional therapy.

Table 5  
Pharmacokinetic parameter of EST loaded nanoparticles

Pharmacokinetic parameter	EST solution	EST CP	EST PNP
A1 (1/h)	-	65719.12	16099.1
Alpha (1/h)	-	14.46	14.6
B (ng/mL)	-	745.59	809.03
Beta (1/h)	-	0.3	0.24
T1/2 alpha (h)	0.509	0.0479	0.0474
T1/2 beta (h)	-	2.305	2.819
Vss (µg/(ng/ml))	0.4	0.1432	0.0569
Cl ((µg)/(ng/ml)/h)	0.544	0.0601	0.057
AUC <sub>0-inf</sub> (ng/ml*h)	458.8714311.71	7022.61	
MRT (h)	0.73	1.21	0.9878

A1: concentration in distribution phase,

a: rate constant of drug elimination from the central compartment including both

elimination from the body and distribution to other compartment,

B: concentration in combined phase,

b: rate constant of drug elimination from the body once the

distribution is complete in a 2-compartment model,

$t_{1/2a}$ : distribution half-life,

$t_{1/2b}$ : physiologic half- life and represents combined effects of distribution and elimination in

2-compartment model,

$V_{ss}$ : apparent Volume of distribution at steady state,

$AUC_{0-\infty}$ : area Under the Curve from time 0 to infinity, and

MRT: mean residence time.

## 4.10. In vivo toxicity studies

Acute toxicity study was conducted to evaluate the adverse effect on single dosing of polymeric nanoparticle in rodents. The animals were observed for any critical, early toxic effects for over a period of 14 days. There was no abnormality or mortality observed in animals in the study period. The organ weights of treated animals were not significantly different ( $P \geq 0.05$ ) from that of control group (fig .7). Normal serum levels of alkaline phosphatase, creatinine, bilirubin, albumin and acceptable levels of complete blood counts like WBC, RBC, lymphocytes, monocytes were obtained. There was no evidence of any artefacts or abnormality in histological sections of vital organs which further reaffirmed the non toxic nature of polymeric nanoparticles (Fig. 8). It was imperative to determine the safety of polymeric nanoparticles with PEI due to the cytotoxicity reportedly associated with this cationic polyamine. Molecular weight, degree of branching and zeta potential govern the toxicity of PEI. In the present work, the concentration of PEI in formulations is within the safety levels, below the LD 50 values reported in animals. Based on the hematological and histological findings it is concluded that the concentration of PEI present in novel polymeric system is safe in vivo.

### 4.11 Biodistribution of polymeric nanoparticles

#### 4.11.1 Radiolabelling of nanoparticles.

Radiolabelling of nanoparticles involved two steps. Firstly, sodium pertechnetate was converted to technitium using stannous chloride reducing agent. This was followed by addition of formulation and incubation in order to facilitate interaction with technitium for efficient radiolabelling.

Since the reaction conditions have a paramount influence on the radiolabeling efficiency, pH, radioactive dose and stannous chloride concentration were optimised. The radiolabelling efficiency was found to be 98-99% which could be attributed to increased binding of negatively charged technetium to a positively charged polymeric surface.

#### **4.11.2 Invasive biodistribution study**

Spatial and temporal in vivo behavior of radiolabelled polymeric nanoparticles was studied. Polymeric nanoparticles were radiolabelled and administered intravenously to mice. Rapid substantial uptake by primary site, RES organs such as liver and spleen, compared to other organs was evident in Fig. 9. Surface hydrophilicity bestowed upon polymeric nanoparticles by poloxamer stabilizer is expected to aid in evasion of opsonisation and further macrophage uptake. However, interplay of other factors such as surface charge and particle size also govern RES uptake, phagocytosis and thereby in vivo biodistribution. In the present investigation, polymeric particles with an average particle size of 178 nm showed significant uptake in liver and spleen. This could be because of the retention of 150-300 nm sized polymeric nanoparticles via filtration in these highly perfused organs which have 150 nm fenestration cut off size (Gaumet, Vargas et al. 2008). Hence larger polymeric nanoparticles with an average particle size of 178 nm are not expected to escape vasculature, instead get entrapped within liver and spleen. Whereas particles smaller than 150 nm escape via filtration. This is reflected in high radioactive RES organ uptake. This observation is in agreement with a number of reports (Vargas et al). There are reports stating that cationic particles have higher propensity to sequestration by RES organs compared to negative or neutral nanoparticles. This could be attributed to higher interaction of cationic nanoparticles with anionic cell membranes thereby leading to phagocytosis and RES uptake. This was distinctly evident from radioactive uptake data in spleen as shown in Fig. 9. However cationic nanoparticles displayed lower hepatic disposition vis-à-vis negatively charged conventional polymeric PLGA nanoparticles. This discrepancy in biodistribution could be attributed to the nature of opsonin proteins bound to the nanoparticle surface. The composition of nanoparticles and their surface characteristics influence the opsonisation and biodistribution process. The presence of splenic phagocyte specific opsonins on cationic nanoparticles would exhibit more affinity to spleen thereby preferentially sequestered in that organ. Whereas kupffer cell specific opsonins bound to negatively charged PLGA nanoparticles is expected to show predominant uptake in liver. However these observations are contrary to the reports which suggest higher propensity of cationic nanoparticles to accumulate in liver compared to neutral or negative ones (Abraham and Walubo 2005).

Positively charged nanoparticles showed profound increase in radioactive levels in kidney relative to non targeted ones. The endothelial cell lining of glomerular capillaries have fenestrations between 30-100 nm. Moreover, the glomerular basement membrane is anionic which is conducive to bind cationic nanoparticles in circulation (Bennett, Zhou et al. 2008).

In 1 h nearly 4% targeted and non targeted nanoparticles were accumulated in bones. There was gradual reduction in the uptake of non targeted nanoparticles with time. At 24h, 1.5% of non targeted nanoparticles and 6% cationic nanoparticles were retained in bones (Fig. 10). This superior bone binding

observed with targeted nanoparticles could be endowed by the interaction of cationic PEI with negative functional groups of HA ensemble in physiological pH. The initial accumulation observed with non targeted nanoparticles could be attributed to the preferential uptake of 30-150 nm particles by bone marrow. Progressive clearance of accumulated non targeted nanoparticles from bone marrow explains the reduction in bone levels with time. It can be deduced that lack of cationic surface molecules to impart bone binding potential led to low bone retention of non targeted nanoparticles in 24h. The polymeric nanoparticles surface modified with cationic PEI exhibited superior bone binding potential both in vitro and in vivo, corroborating the proposed hypothesis.

#### **4.11.3 Non invasive biodistribution study**

In addition to determining and computing radioactive counts in individual organs, the in vivo fate of developed formulations was evaluated non invasively using SPECT imaging. The superimposed images of CT and SPECT clearly displayed the differences in the intensity of radioactive uptake by organs. These observations commensurate the organ uptake values calculated in invasive study. The images Fig. 11 and 12 depict the uptake of conventional (plain PLGA) nanoparticles and cationic nanoparticles. It was distinctly seen from images that positively charged nanoparticles displayed lower hepatic uptake compared to plain PLGA nanoparticles. This is in agreement with the findings of invasive uptake study.

It is to be noted that the invasive study indicates nearly 5-8 fold higher uptake by liver compared to bones, a less perfused organ. Moreover the distribution of radioactivity calculated in invasive method accounts for the entire skeleton. Hence the SPECT images fail to visually depict the difference in the uptake by bone or different formulations.

#### **4.11.4 In vivo efficacy study**

Surgically ovariectomised rat model is one of the most reliable preclinical evaluation tools to study the effect of hormonal intervention in post menopausal condition. Ovariectomy causes decline in estrogen levels further leading to bone loss. Estrogen therapy reportedly causes improvement in bone density and mechanical properties in ovariectomised rats. In the present work, animals were treated with EST solution and nanoparticles. There was no mortality was observed in any groups during the study period. There was no abnormality in activity and their food intake.

#### **4.12. 1. Mechanical properties**

It is reported that the rat OVX model in the proximal tibia, distal femur, and lumbar vertebrae

mimics conditions in the postmenopausal woman and is suitable for the evaluation of potential

therapeutic agents for the prevention of osteoporosis (Thompson. Simmons et al, 1995). Therefore in the present work, tibia and femur have been isolated and studied for the influence of EST on bone properties. Bone density was determined using Archimedes principle. Comparable hardness and density values of cationic nanoparticles with SHAM operated rats indicate osteoprotective nature of these hormone replacement therapy formulations (figure 13, 14). It implies that there is no significant difference in

osteoprotective activity of natural estrogen (in sham operated rats) and EST in PEI coated nanoparticles. As expected bone density of animals treated with cationic nanoparticles was significantly higher than the OVX control group ( $P < 0.001$ ). Bone strength was evaluated by subjecting a force longitudinally to cause breakage. Bones with hard matrix would require higher force to break the bone. Higher the hardness value, stronger the bone. Bones with low mass and density are more susceptible to fracture. Higher density and hardness values indicate higher bone strength and resistance to bone breakage under force. Solutions were administered intravenously twice / week. The prolonged sustained drug exposure exhibited from targeted nanoparticles vis a vis poor drug bioavailability in solutions. Therefore solutions did not have significant influence in the bone strength.

#### **4.12. 2. Biochemical parameters**

Biochemical parameters such as alkaline phosphatase (ALP), calcium, phosphorous

are biomarkers which reportedly govern changes occurring in bone (Gupta, Goyal et al, 2014). ALP is widely found in bone cells and liver. ALP levels increase in skeletal disorders. In the present study, serum levels were significantly higher in ovx control animals compared to sham control and the rats treated with nanoparticles (Fig. 15.). These results are in agreement with the observations made in ovx females treated with estrogen (Pedrazzoni, Alfano et al, 1995). Alk P levels in formulation treated animals were similar to that of sham control group. However they were significantly lower compared to solution ( $P < 0.001$ ) implying inadequate estrogen levels from solution to aid bone remodeling.

Serum calcium and phosphorus levels were significantly higher in sham control vis a vis ovx control animals ( $P < 0.001$ ) (Fig. 16, 17). Formulations and sham control animals exhibited similar serum calcium and phosphorus levels. Gupta et al reported a similar observation in ovx animals treated with plant extracts. Sustained release of EST from formulations ensured desired therapeutic levels of EST for pronounced osteoprotective activity. Biochemical and mechanical evaluation of EST bone targeted nanoparticles confirm the superior osteotropic and protective action in ovariectomised rats.

## **5. Conclusion**

The novel bone targeted cationic nanoparticles proved to be safe and osteotropic based on in vitro and preclinical evaluation. These systems can be considered a prototype for delivery of plethora of antiresorptive or anabolic agents to the skeletal environment making them pertinent in treating debilitating bone disorders like osteoporosis, Paget's disease, osteomyelitis, bone sarcoma, bone metastasis.

## **Declarations**

### **Ethics approval**

**Animal Studies-** All institutional and national guidelines for the care and use of laboratory animals were followed. We declare that the experiments comply with the current laws of the country in which they were

performed. Ethical approval: All procedures performed in studies involving animals were in accordance with the ethical standards of the institution at which the studies were conducted and ethical approval was obtained from Institutional Animal Ethics Committee (IAEC), CPCSEA-BCP/2016-01/18.

This article does not contain any studies with human participants performed by any of the authors.

**Consent to participate-** Not applicable

**Consent to publish-** Not applicable

**Availability of data and materials-** *The datasets generated during and/or analysed during the current study are available from the corresponding author on reasonable request*

**Competing interest-** *The authors have no relevant financial or non-financial interests to disclose.*

**Conflict of interest-** Authors declare that they have no conflict of interest.

**Funding:** The research work was funded by Department of Science and Technology (DST), Nanomission-SR/NM/NS-1103-2011.

#### **Author contribution-**

Meenakshi Venkataraman- 1. Made substantial contributions to the conception and design of the work; 2. Contributed to acquisition, analysis, and interpretation of data; 3. drafted and revised work critically

Bhabani Mohanty , Pradip Chaudhari and Darshan Kumar- Contributed to experimentation and data analysis

Mangal Nagarsenker- Critical revision of the manuscript. Agree to be accountable for all aspects of the work in ensuring that questions related to the accuracy or integrity of any part of the work are appropriately investigated and resolved.

#### **Acknowledgements**

Authors would like to thank BASF for providing gift sample of poloxamer 188. Authors would like to acknowledge the contributions of veterinarians Dr. Chaudhary, Dr. Gaurav and Dr. Abhijeet for their inputs in animal studies.

**Authors information-** Meenakshi Venkataraman <sup>a</sup>, Bhabani Mohanty <sup>b</sup>, Pradip Chaudhari <sup>b</sup>, Darshan Kumar <sup>c</sup>, Mangal Nagarsenker <sup>d</sup>

Meenakshi Venkataraman, PhD

**Email id-** meenakshiv2412@gmail.com

Affiliation-Bombay College of Pharmacy,Kalina, Santacruz (E),  
Mumbai 400 098. India

Bhabani Mohanty email id – bhabani.bmohanty@gmail.com and Pradip Chaudhari- email id-  
pchaudhari@actrec.gov.in. Advance Centre for Treatment Research & Education in Cancer, Tata Memorial  
Centre, (ACTREC), Plot No. 1 & 2, Sector 22, Kharghar, Navi Mumbai-410210. Maharashtra India.

Darshan Kumar Department of Biotechnology, Vilkincaari 5, University of Helsinki

**Corresponding author-** Dr. (Mrs.) Mangal Nagarsenker,

Research Advisor at VES institute of Pharmacy,

Retd Prof and HOD at Bombay College of Pharmacy,

Kalina. Santacruz East

Mumbai-400098

Email id- [mangal.nagarsenker@gmail.com](mailto:mangal.nagarsenker@gmail.com).

Ethics approval and consent to participate:

- o Consent for publication:
- o Availability of data and materials:
- o Competing interests:
- o Funding:
- o Authors' contributions:
- o Acknowledgements:

## References

1. Abraham, A. and A. Walubo (2005). "The effect of surface charge on the disposition of liposome-encapsulated gentamicin to the rat liver, brain, lungs and kidneys after intraperitoneal administration." International journal of antimicrobial agents**25**(5): 392-397.
2. Bennett, K. M., H. Zhou, J. P. Sumner, S. J. Dodd, N. Bouraoud, R. A. Star and A. P. Koretsky (2008). "MRI of the basement membrane using charged nanoparticles as contrast agents." Magnetic resonance in medicine**60**(3): 564-574.
3. Gu, P, Wusiman. A, Zhang. Y, Liu. Z, Bo. R, Hu. Y, Liu. J, Wang. D. 2019. Rational design of PLGA nanoparticle vaccine delivery systems to improve immune responses. *Mol. Pharm.* **16**, 5000–5012. DOI: [10.1021/acs.molpharmaceut.9b00860](https://doi.org/10.1021/acs.molpharmaceut.9b00860)
4. Gelperina, S., O. Maksimenko, A. Khalansky, L. Vanchugova, E. Shipulo, K. Abbasova, R. Berdiev, S. Wohlfart, N. Chepurnova and J. Kreuter (2010). "Drug delivery to the brain using surfactant-coated

- poly (lactide-co-glycolide) nanoparticles: influence of the formulation parameters." European Journal of Pharmaceutics and Biopharmaceutics**74**(2): 157-163.
5. Gupta, R., Goyal. R, Bhattacharya. S., Dhar, K. L. (2014). " Antioxidative in vitro and antiosteotropic activities of *Prinsepia utilis* Royle in female rats." European Journal of Integrative medicine. <http://dx.doi.org/10.1016/j.eujim.2014.10.002>
  6. Hirabayashi, H. and J. Fujisaki (2003). "Bone-specific drug delivery systems." Clinical pharmacokinetics**42**(15): 1319-1330.
  7. Jose. S, Cinu. T.A, Sebastian. R, Shoja. M. H, Aleykutty. N.A, Durazzo. A, Lucarini. M, Santini. A, Soulo. E.B. 2019. Transferrin-conjugated docetaxel-PLGA nanoparticles for tumor targeting: influence on MCF-7 cell cycle. Polymers **11**, 1905. doi: [10.3390/polym11111905](https://doi.org/10.3390/polym11111905)
  8. Khosla. S., Oursler. M.J., Monroe. D.G (2012). "Estrogen and the Skeleton". Trends Endocrinol Metab. 2012 November ; **23**(11): 576–581. doi:[10.1016/j.tem.2012.03.008](https://doi.org/10.1016/j.tem.2012.03.008).
  9. Kong, W. N. G., Romas, E., Donnan, L., Findlay, D. M., 1997. Bone biology. Baillidre's Clinical Endocrinology and Metabolism. **11**, No. 1.
  10. Li, X., Y. Xu, G. Chen, P. Wei and Q. Ping (2008). "PLGA nanoparticles for the oral delivery of 5-Fluorouracil using high pressure homogenization-emulsification as the preparation method and in vitro/in vivo studies." Drug development and industrial pharmacy**34**(1): 107-115.
  11. Meng-Xia Ji, Qi Yu. 2015. Primary osteoporosis in postmenopausal women. Chronic diseases and translational medicine.**1**, 9-13. <https://doi.org/10.1016/j.cdtm.2015.02.006>.
  12. Mitchell, M. J, Billingsley. M. M., Haley. R. M., Wechsler. M. E., Nicholas A. Peppas. N.A., Langer.R. (2021) . Engineering precision nanoparticles for drug delivery. Nature Reviews Drug Discovery. **20**, 101–124. <https://doi.org/10.1038/s41573-020-0090-8>
  13. Mittal, G., D. Sahana, V. Bhardwaj and M. R. Kumar (2007). "Estradiol loaded PLGA nanoparticles for oral administration: effect of polymer molecular weight and copolymer composition on release behavior in vitro and in vivo." Journal of Controlled Release**119**(1): 77-85.
  14. Musumeci, T., C. A. Ventura, I. Giannone, B. Ruozi, L. Montenegro, R. Pignatello and G. Puglisi (2006). "PLA/PLGA nanoparticles for sustained release of docetaxel." International journal of pharmaceutics**325**(1): 172-179.
  15. Patere. S. N., Pathak. P. O., Shukla. A.K., Singh. R. K., Dubey. V. K., Mehta. M. J., Patil. A. G., Gota. V., Nagarsenker. M. S. 2016. Surface-Modified Liposomal Formulation of Amphotericin B: In vitro Evaluation of Potential Against Visceral Leishmaniasis. AAPS PharmSciTech DOI: [10.1208/s12249-016-0553-8](https://doi.org/10.1208/s12249-016-0553-8)
  16. Pedrazzoni, M., Alfano. F.S., Girasole. G., Giuliani. N., Fantuzzi.M., Gatti.C., Campanini,C., Passeri,M.( 1996). "**Clinical Observations with a New Specific Assay for Bone Alkaline Phosphatase: A Cross-Sectional Study in Osteoporotic and Pagetic Subjects and a Longitudinal Evaluation of the Response to Ovariectomy, Estrogens, and Bisphosphonates**". Calcified Tissue International **59**:334–338

17. Peterlik, M., 1997. Aging, neuroendocrine function, and osteoporosis. *Exp Gerontol.* 32, 577-586. doi: 10.1016/s0531-5565(96)00160-x
18. Pivonka, P., Zimak, J., Smith, D. W., Gardiner, B. S., Dunstan, C.R., Sims, N. A., Martin, T. J., Mundy, G. R., 2008. Model structure and control of bone remodeling: A theoretical study. *Bone.* 43, 249–263. doi: 10.1016/j.bone.2008.03.025
19. Shahzad, K. A, Naeem. M, Zhang. L, Wan. X, Song. S, Pei. W, Zhao. C, Zhao. C, Jin. X, Shen. C. 2019. Design and optimization of PLGA particles to deliver immunomodulatory drugs for the prevention of skin allograft rejection. *Immunol. Invest.* 49, 840–857 (2019). doi: 10.1080/08820139.2019.1695134.
20. Shea, J. E. and S. C. Miller (2005). "Skeletal function and structure: implications for tissue-targeted therapeutics." *Advanced drug delivery reviews***57**(7): 945-957.
21. Thompson, D. D, Simmons, H. A, Pirie. C. M, Ke. H. Z (1995). "FDA guidelines and animal models for osteoporosis" *Bone* 17 (4): 125S-133S.
22. Venkataraman. M, Nagarsenker. M. 2013. Silver sulfadiazine nanosystems for burn therapy. *AAPS PharmSciTech.* 14, 254-64. doi: 10.1208/s12249-012-9914-0.
23. Wang, D., Miller, S.C., Kopecká, P., Kopeček, J., 2005. Bone-targeting macromolecular therapeutics. *Adv Drug Deliv Rev.* 57, 1049– 1076. doi: 10.1016/j.addr.2004.12.011.
24. Yan, F., C. Zhang, Y. Zheng, L. Mei, L. Tang, C. Song, H. Sun and L. Huang (2010). "The effect of poloxamer 188 on nanoparticle morphology, size, cancer cell uptake, and cytotoxicity." *Nanomedicine: Nanotechnology, Biology and Medicine***6**(1): 170-178.
25. Yoo, J.-W. and C. H. Lee (2006). "Drug delivery systems for hormone therapy." *Journal of controlled release***112**(1): 1-14.
26. Zhang, S., J. E. Wright, N. Özber and H. Uludağ (2007). "The interaction of cationic polymers and their bisphosphonate derivatives with hydroxyapatite." *Macromolecular bioscience***7**(5): 656-670.

## Figures

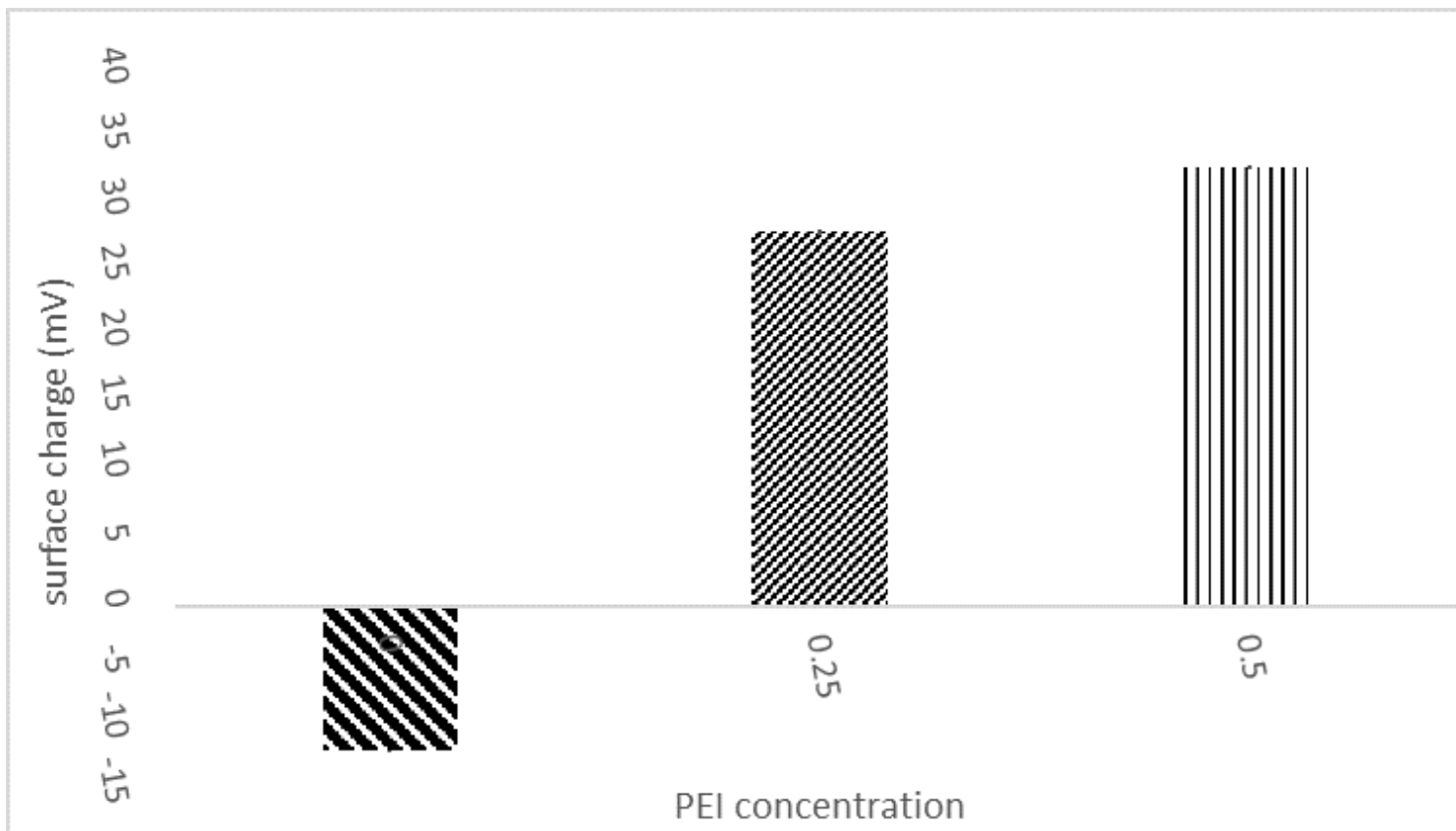


**Figure 1**

Influence of PEI concentration (% w/w) on surface charge of nanoparticles

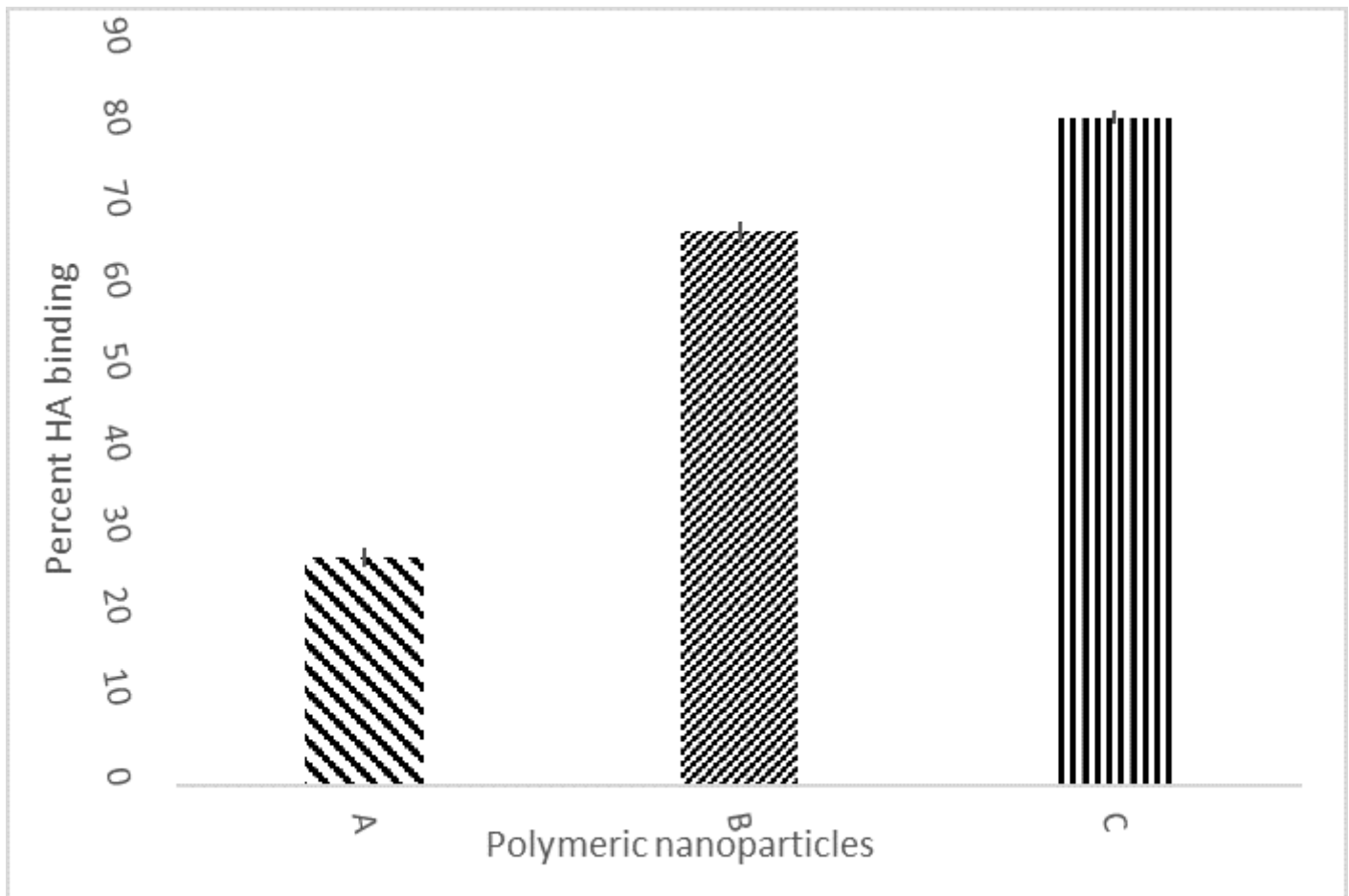


**Figure 2**

*In vitro* HA binding affinity of polymeric nanoparticles

Wherein, A-0 % w/w PEI, 2.5 %w/w PEI, 5% w/w PEI

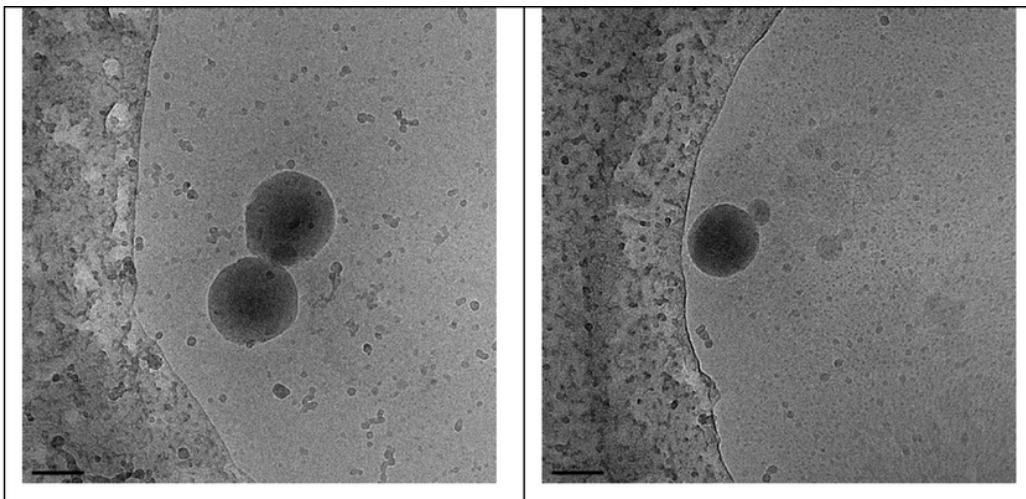
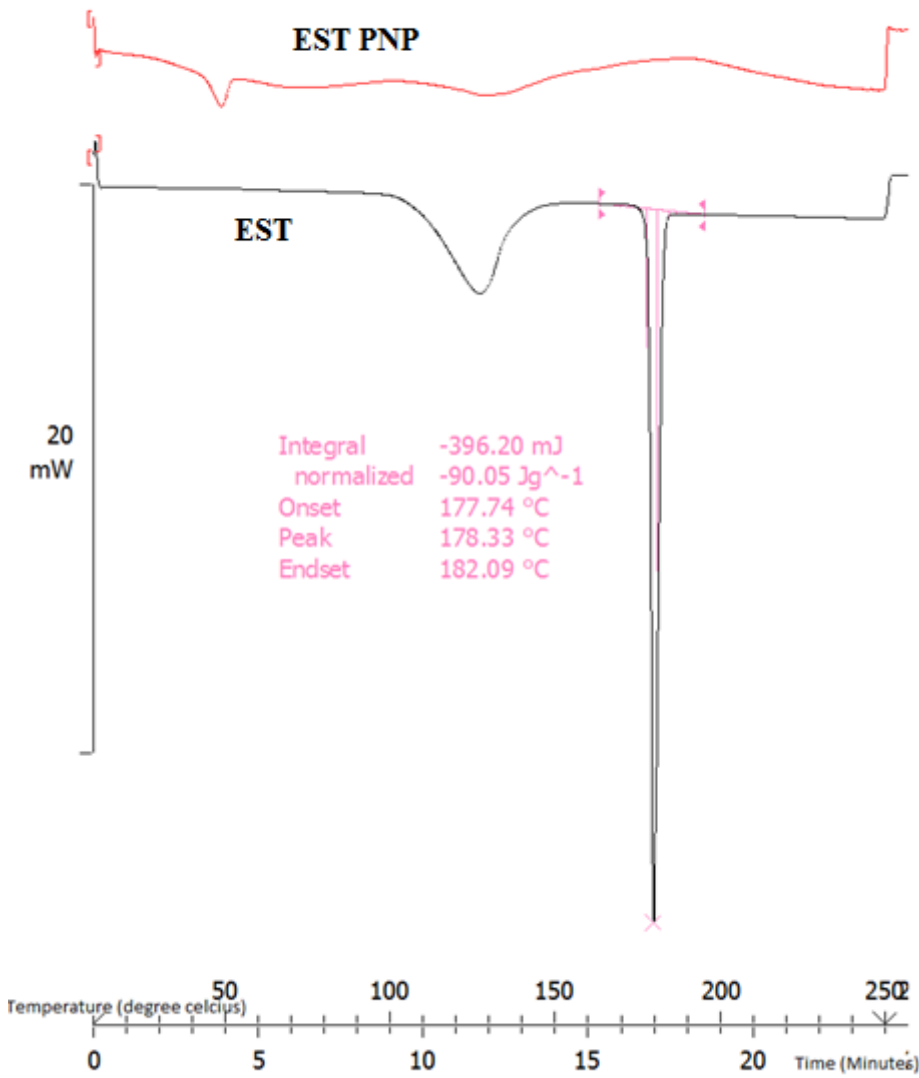


Figure 3

Cryo TEM images of cationic PEI coated polymeric nanoparticles

exo



Bombay College of Pharmacy: METTLER

Figure 4

DSC thermogram of EST and EST cationic polymeric nanoparticle

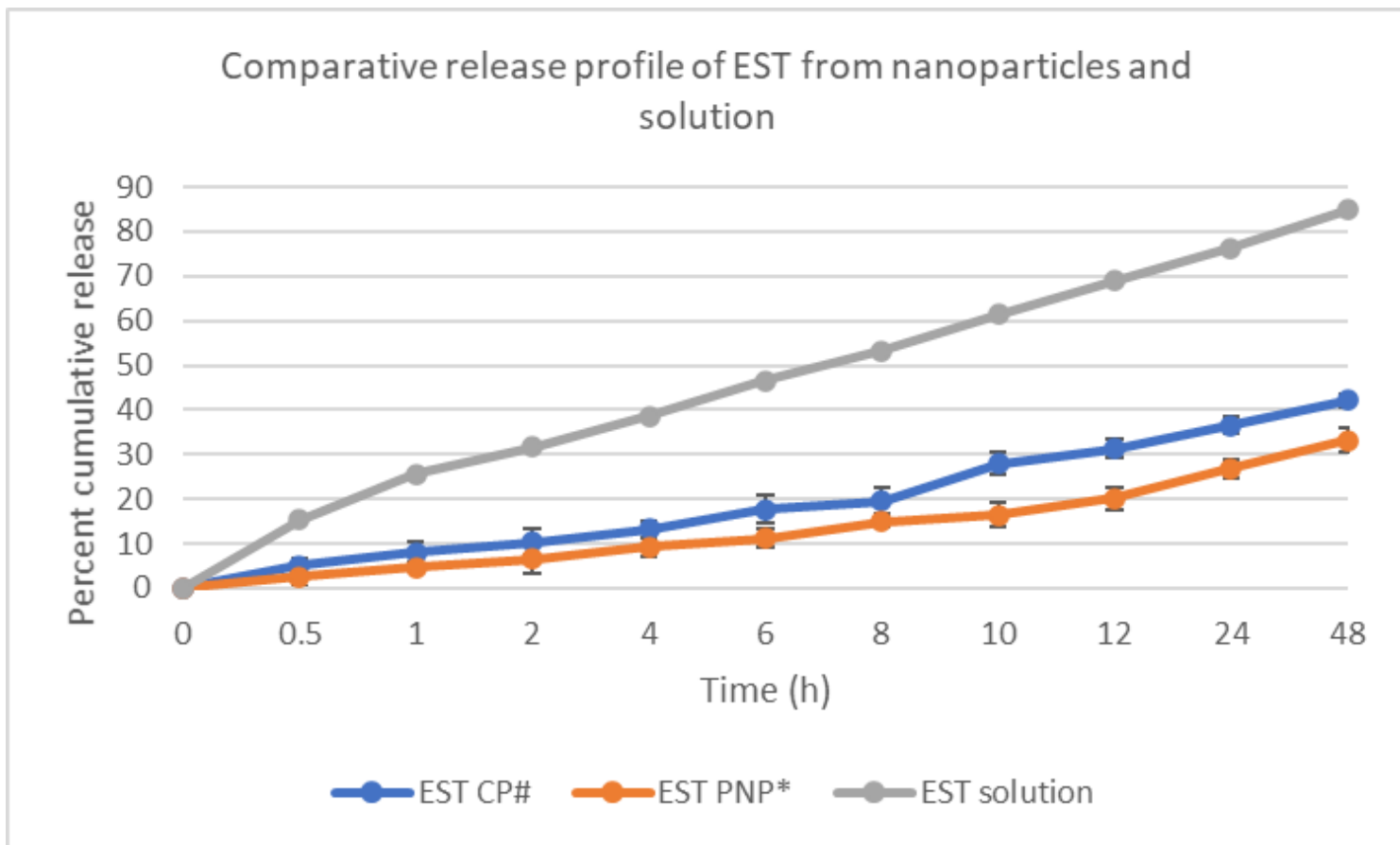


**Figure 5**

Comparative release profile of EST nanoparticles and solution

#EST CP- Estradiol loaded conventional plain PLGA nanoparticles,

\* EST PNP – Estradiol loaded PEI coated polymeric nanoparticles

EST solution-Estradiol solution

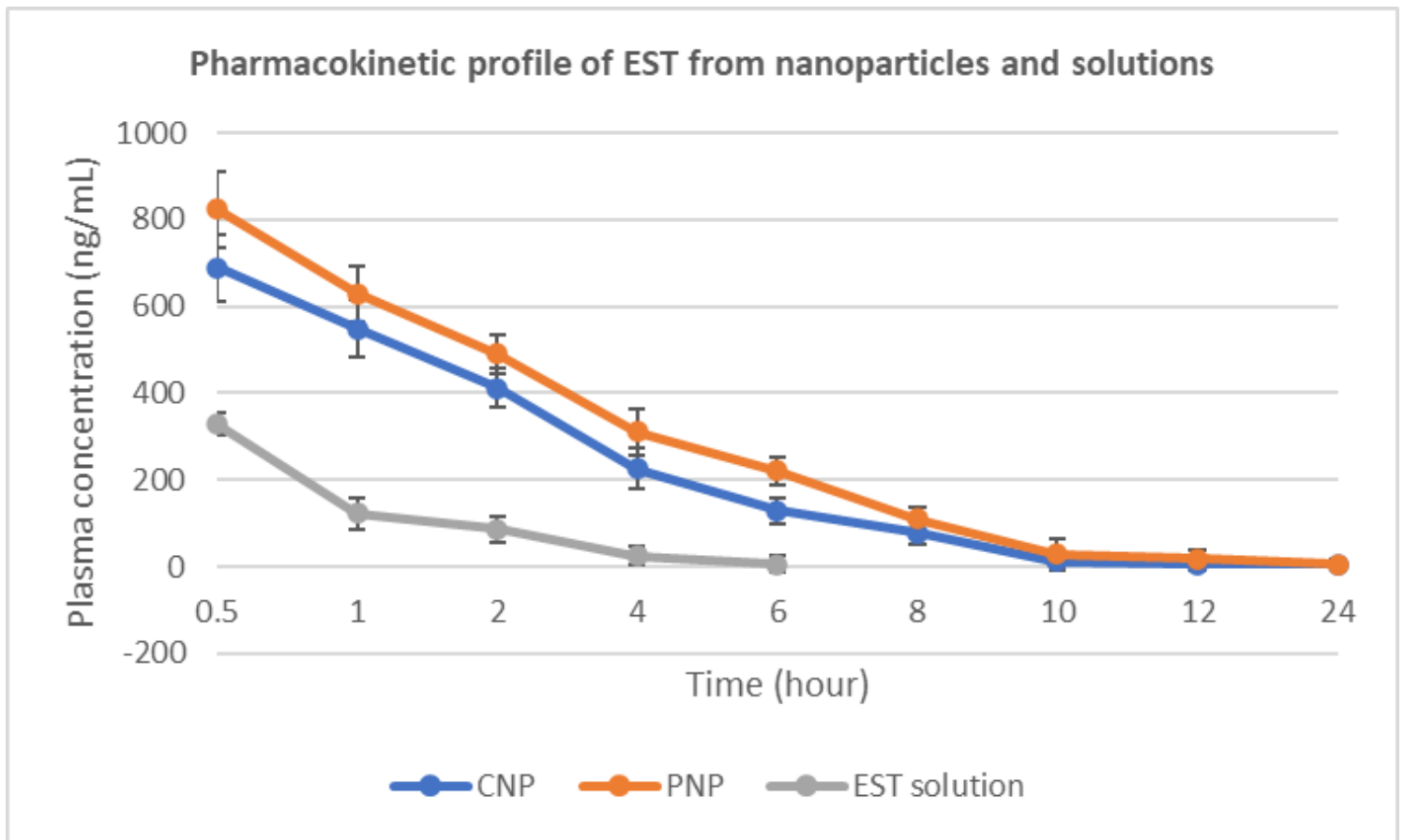
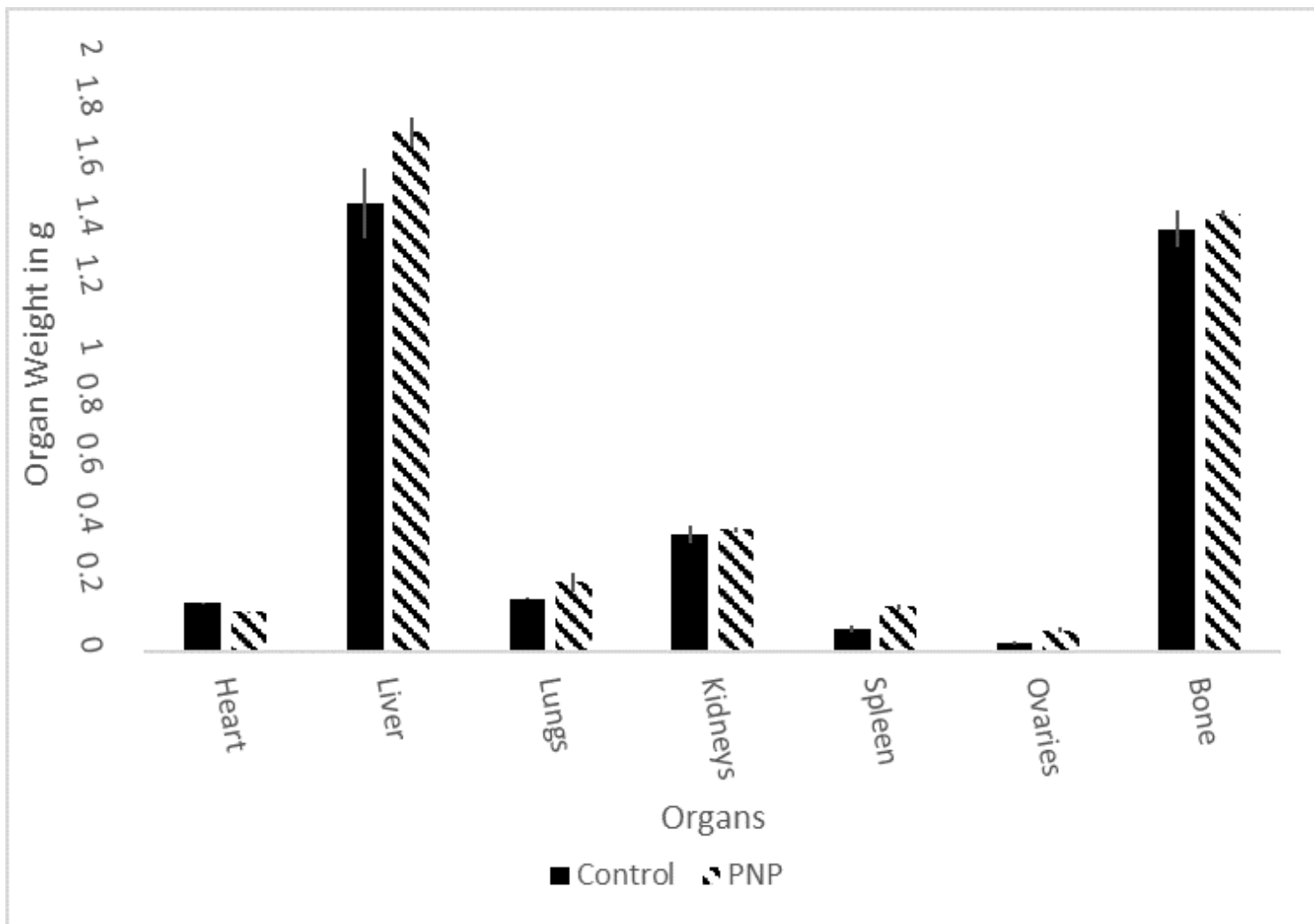


Figure 6

Pharmacokinetic profile of EST from nanoparticles and solution



**Figure 7**

Organ weights- control group vis-à-vis cationic nanoparticle treated animals

	<b>Heart</b>	<b>Lungs</b>	<b>Liver</b>	<b>Bone Marrow</b>	<b>Spleen</b>	<b>Ovary</b>
<b>Control</b>						
<b>Polymeric nanoparticles</b>						

**Figure 8**

Histological sections of organs (control vis-à-vis cationic nanoparticles)

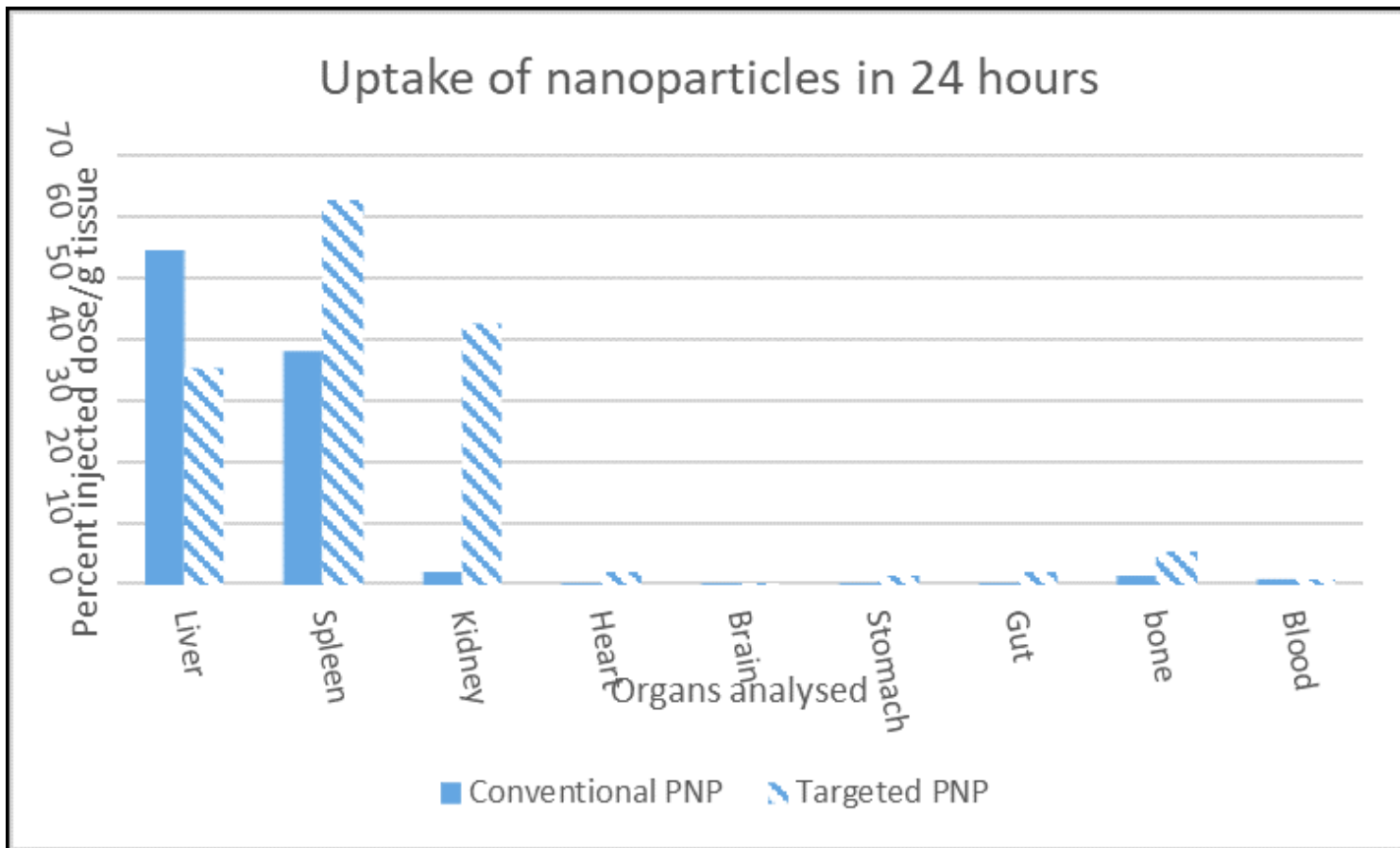


**Figure 9**

Uptake of nanoparticles in 24 hours

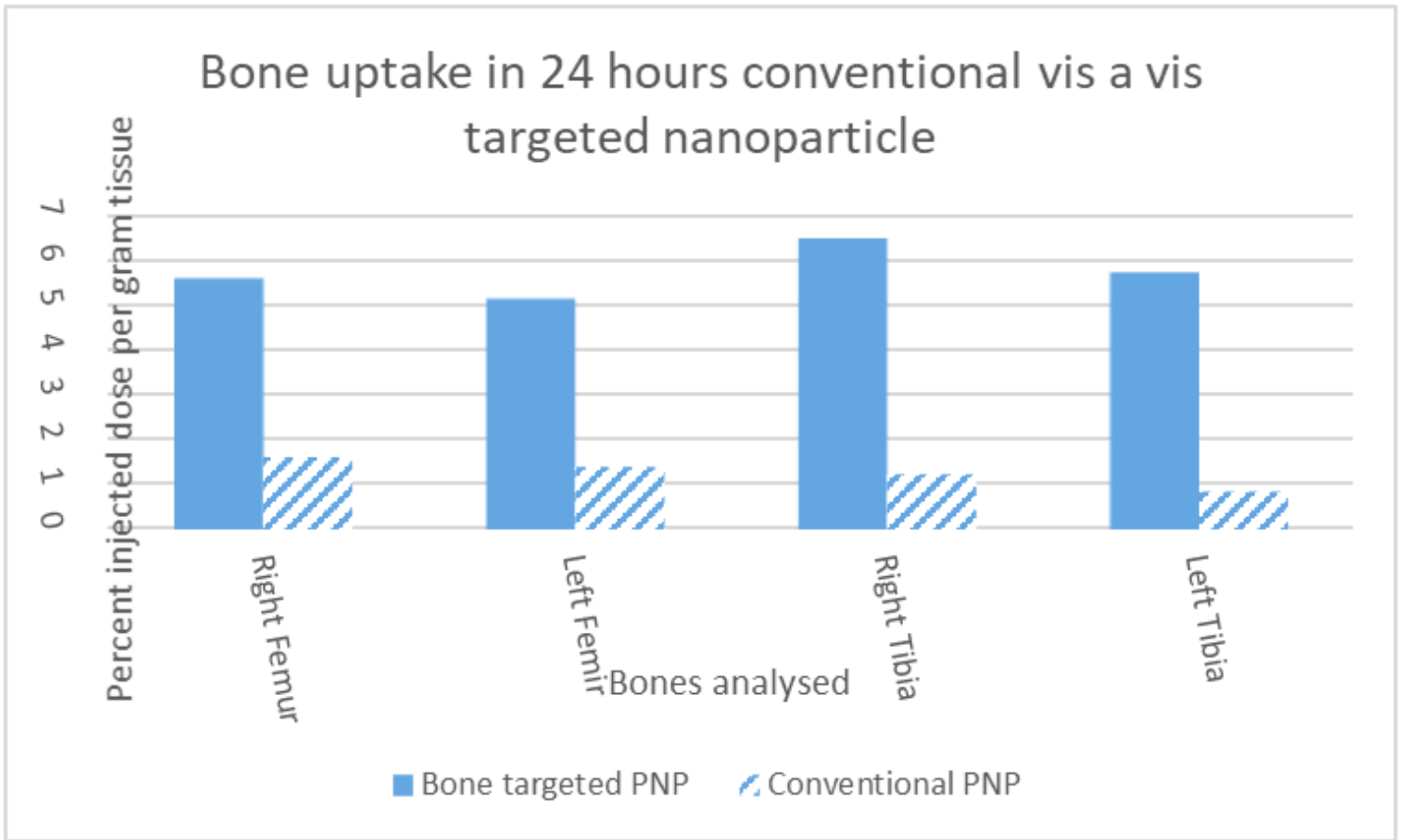


**Figure 10**

Bone uptake in 24 hours conventional vis a vis targeted nanoparticle

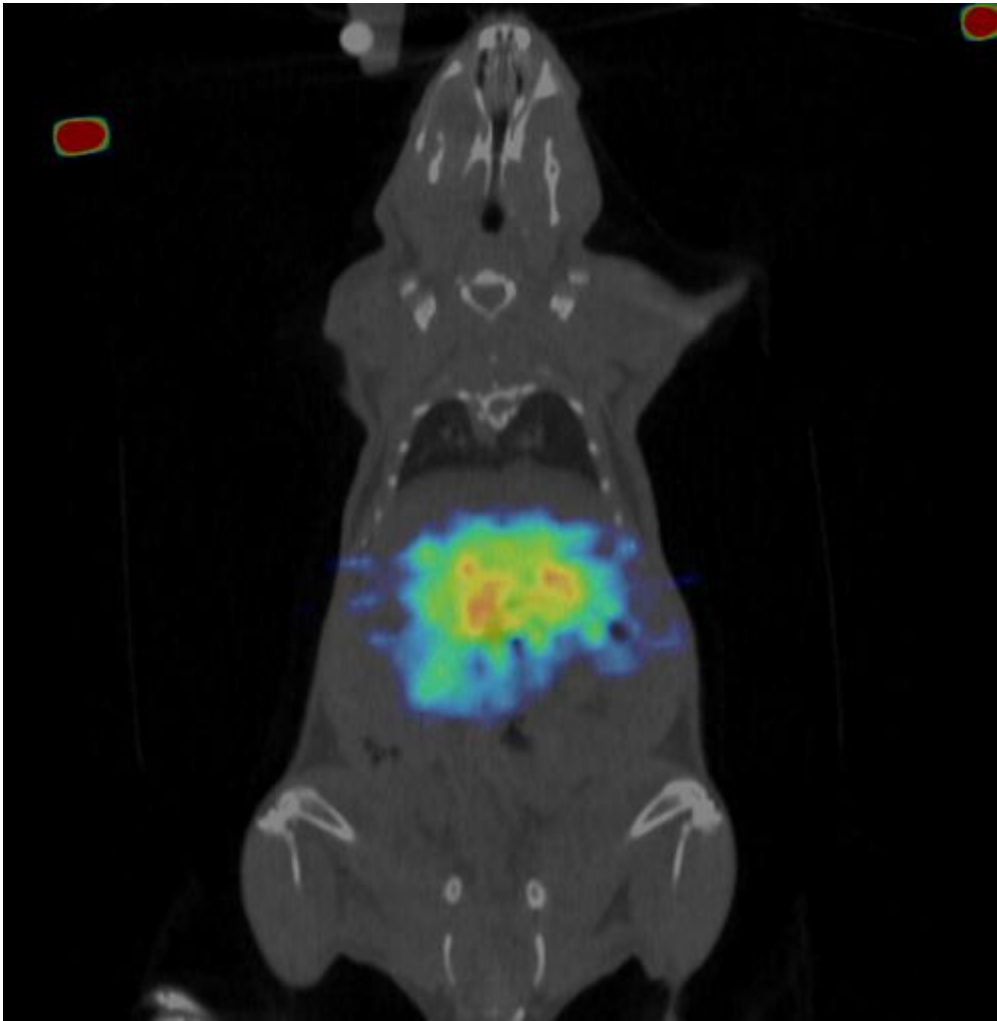


**Figure 11**

Representative SPECT image depicting biodistribution of conventional nanoparticles

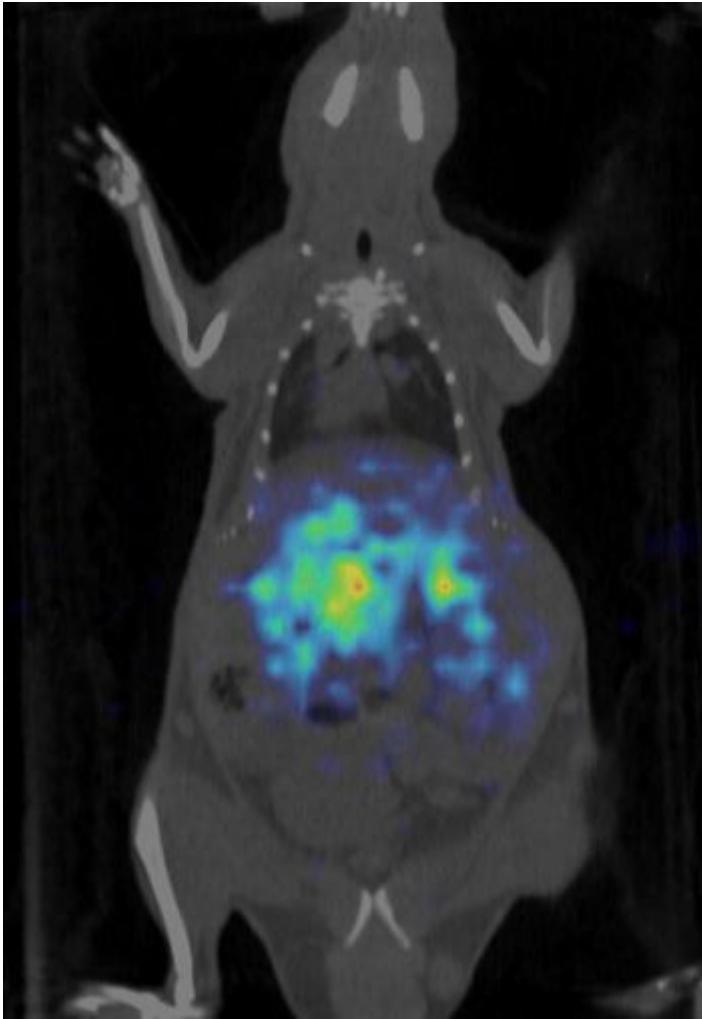


**Figure 12**

Representative SPECT image depicting biodistribution of Cationic polymeric nanoparticles

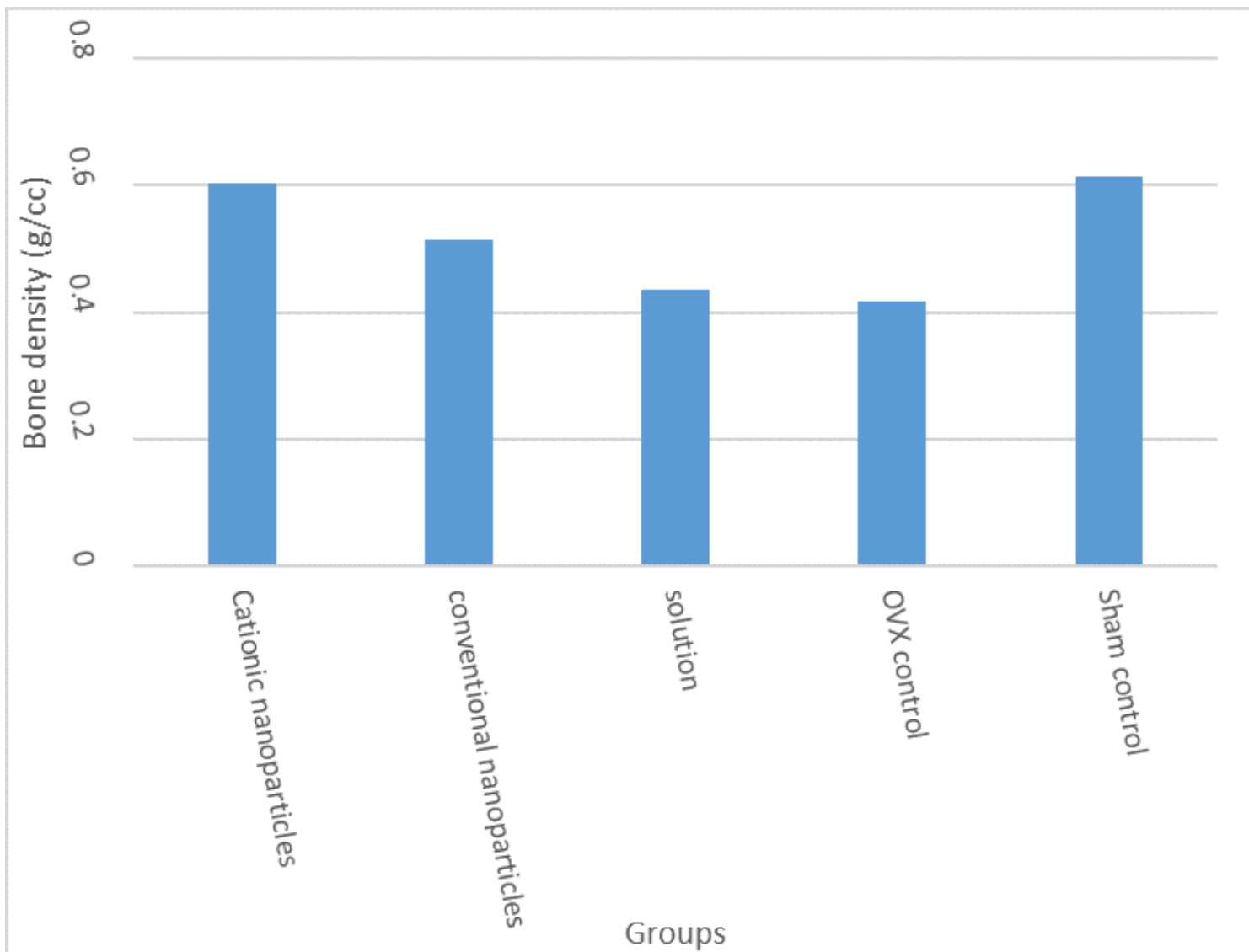


**Figure 13**

Graph depicting bone density values

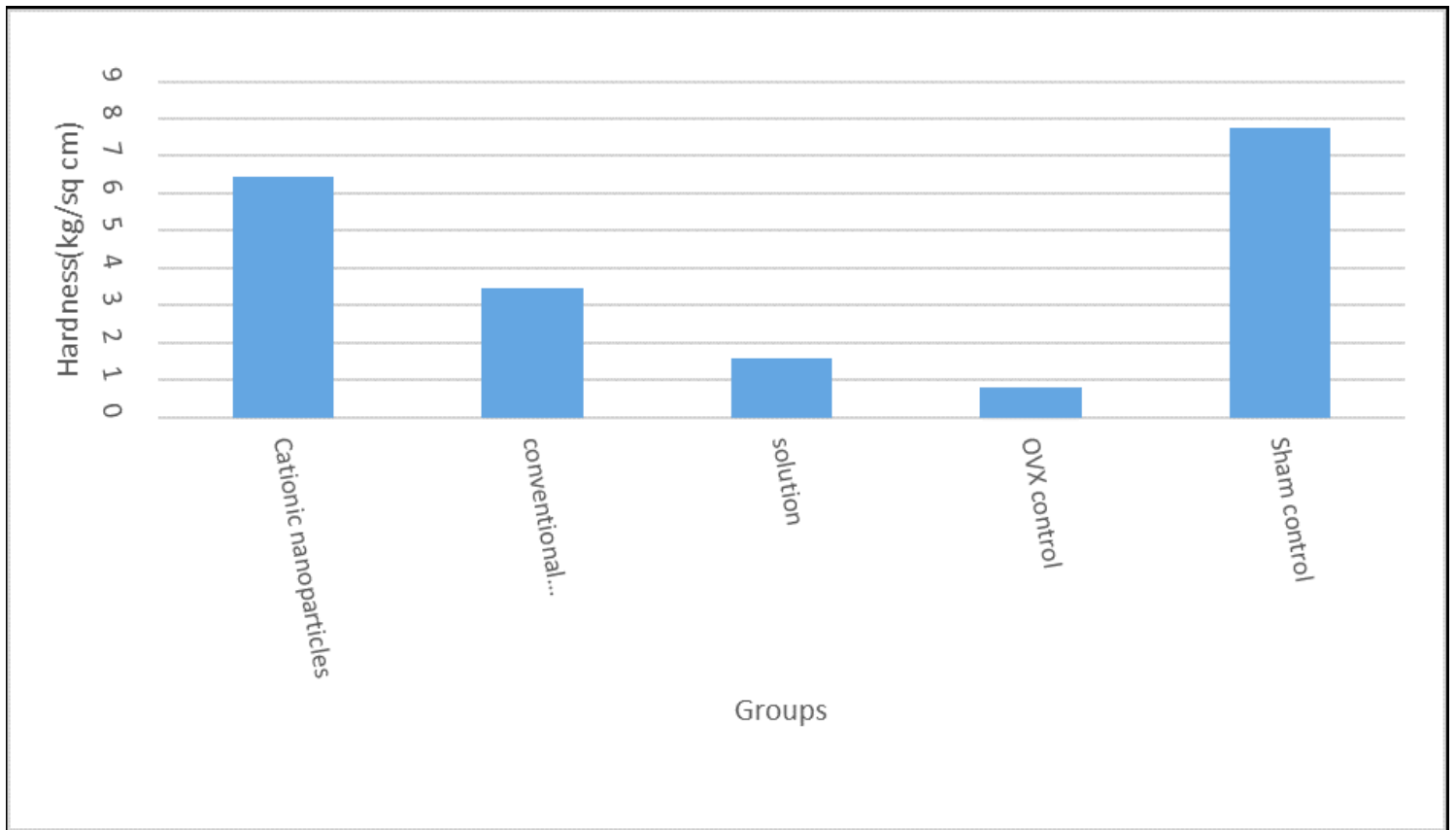


**Figure 14**

Graph depicting hardness values

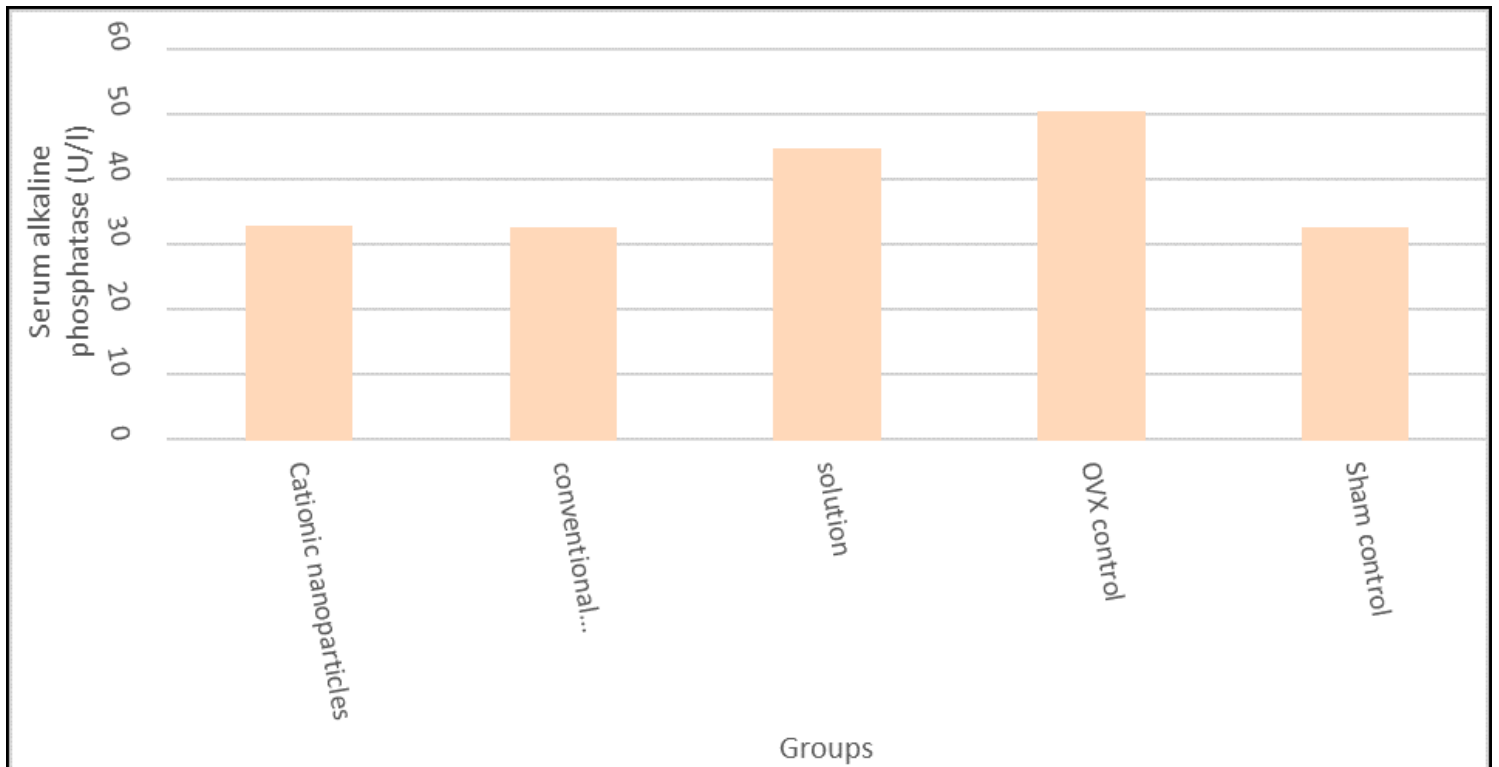


**Figure 15**

Graph depicting serum alkaline phosphatase levels

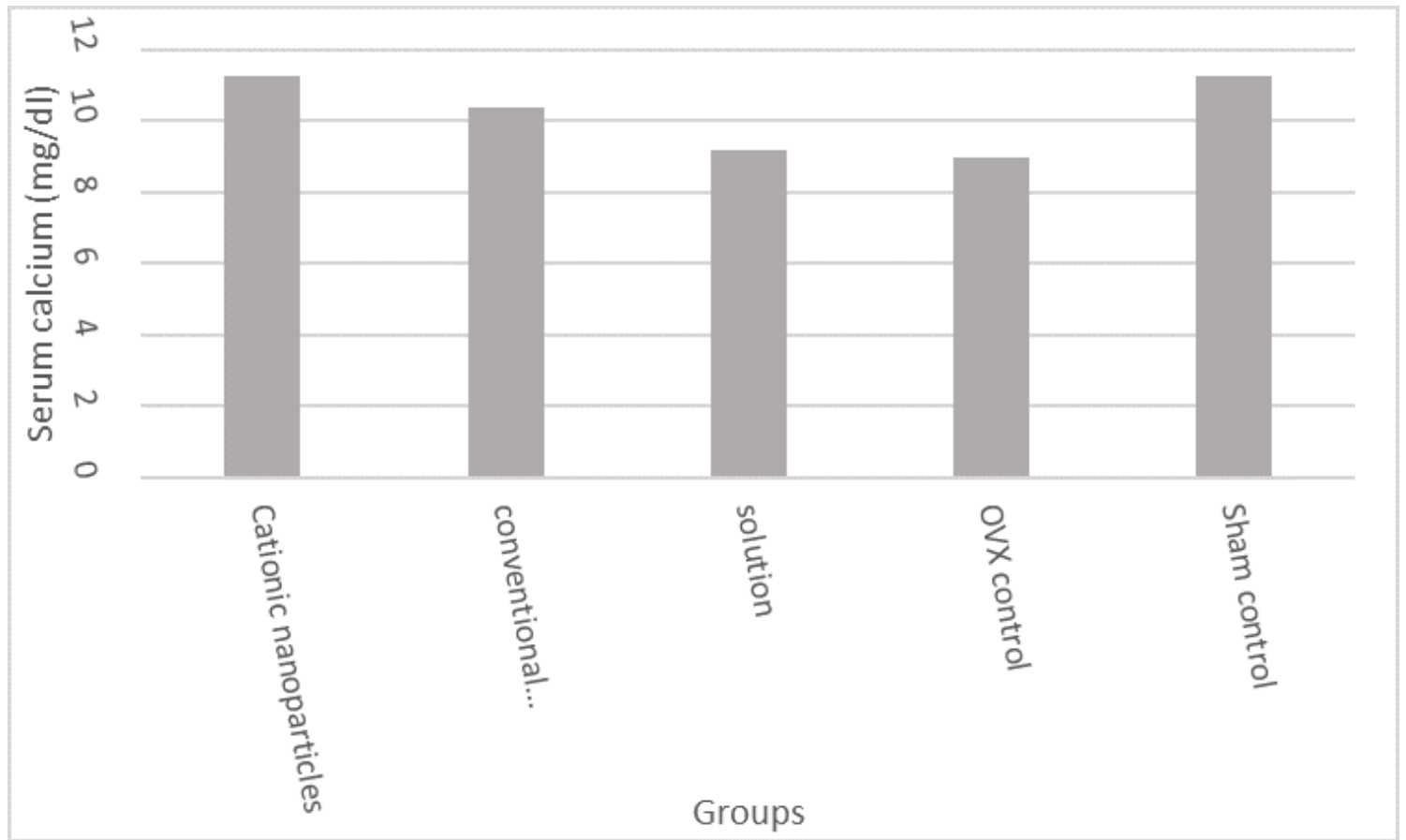


**Figure 16**

Graph depicting serum calcium levels

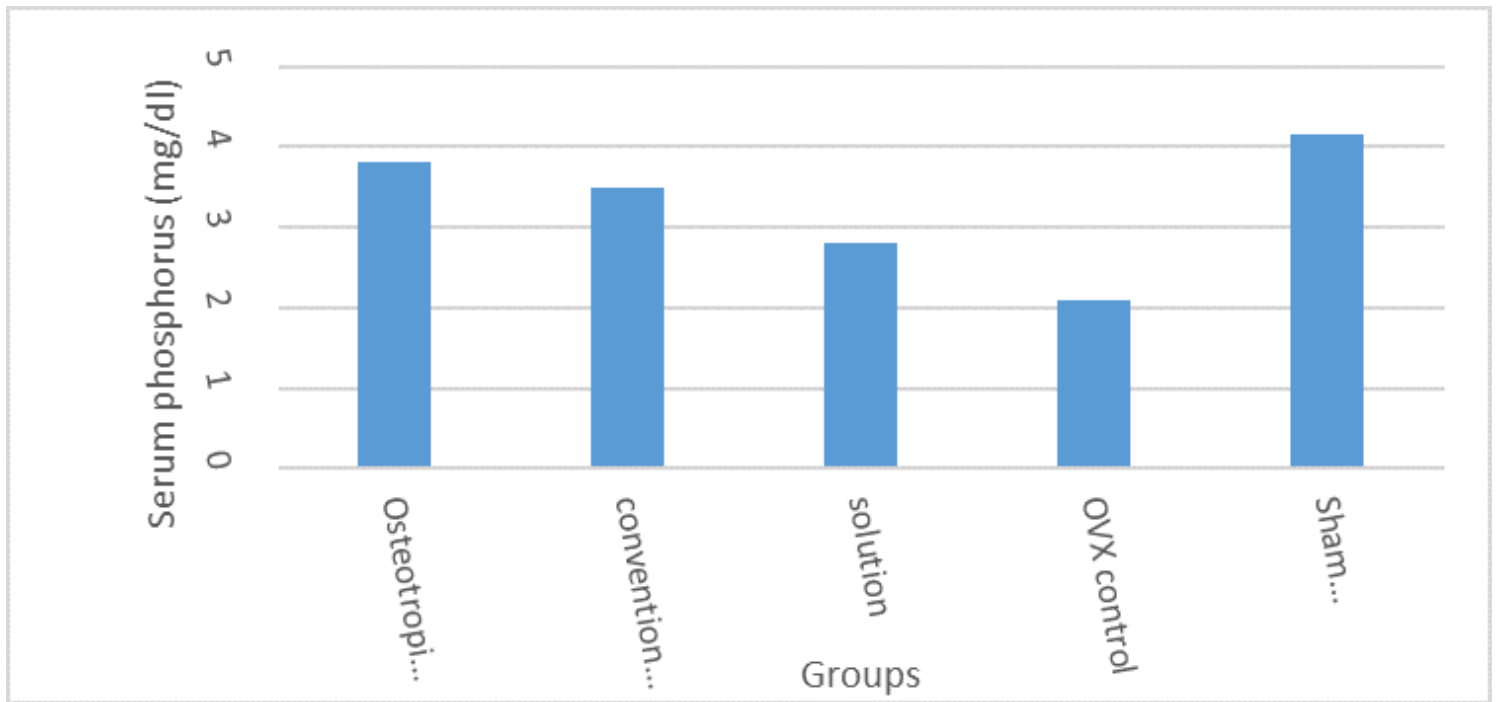


Figure 17

Graph depicting serum phosphorus levels

## Supplementary Files

This is a list of supplementary files associated with this preprint. Click to download.

- [floatimage1.png](#)